ENCAPSULATION OF LUMINESCENT POLYMERS IN POROUS ALUMINA

by

Keri Kwong

B. Sc., University Of Toronto, 1999

A THESIS SUBMITTED IN PARTIAL FULFILMENT OF
THE REQUIREMENTS FOR THE DEGREE OF

MASTER OF SCIENCE

IN

THE FACULTY OF GRADUATE STUDIES

(Department of Chemistry)

We accept this thesis as conforming
to the required standard

THE UNIVERSITY OF BRITISH COLUMBIA

SEPTEMBER 2001

© Keri Kwong, 2001

In presenting this thesis in partial fulfilment of the requirements for an advanced degree at the University of British Columbia, I agree that the Library shall make it freely available for reference and study. I further agree that permission for extensive copying of this thesis for scholarly purposes may be granted by the head of my department or by his or her representatives. It is understood that copying or publication of this thesis for financial gain shall not be allowed without my written permission.

Department of Chemistry

The University of British Columbia
Vancouver, Canada

Date Sept. 28th 2001

Abstract

The incorporation of three conjugated polymers: MEH-PPV, DP-PPV and DP_{10}-PPV into porous alumina films on Al, Si and ITO substrates via an adsorption process is reported. The nature of this adsorption process involves bonding between Lewis acidic Al centres on the alumina and the Lewis basic polymer backbone. The MEH-PPV porous alumina hybrids was found to degrade rapidly upon the irradiation of UV-light (λ_{ext} = 366 nm) in air but to a lesser extent in the dark and under nitrogen. Silanization of the pores by treatment with trimethylchlorosilane (TMS), phenyldimethylchlorosilane (PDMS) and octyldimethylchlorosilane (ODMS) resulted in lower MEH-PPV loading in porous alumina membranes (Anodisc 13) relative to the membranes with unmodified pore walls. In the fluorescence spectra, the intensity of the fluorescence from the Anodisc membranes containing MEH-PPV is higher than from MEH-PPV in silanized porous alumina. The Lewis acidic Al centres of the porous alumina in the silanized pores are screened from the Lewis basic polymer resulting in a lower fluorescence intensity. Within the silanes used, the absorbance intensity is in the order: TMS > ODMS, PDMS. Within the silanes, the difference in fluorescence intensities may be due to the size of the alkyl/aryl groups. The larger alkyl substituent in ODMS and the aryl group in PDMS may act to better screen the Lewis acidic Al than in the smaller alkyl group in TMS. In DP_{10}-PPV, the unmodified porous alumina has a higher fluorescence intensity relative to the modified materials. This is attributed to the interactions between the pore walls and the polymer. The same screening effect that occurs for MEH-PPV is also observed for DP_{10}-PPV. For DP_{10}-PPV, the fluorescence intensities is in the order: PDMS > ODMS,

TMS. This difference may arise from the favourable π-stacking interactions between the polymer and the PDMS silanized pores.

Table of Content

Abstract.....ii
Table of Contents.....iv
List of Schemes.....vi
List of Figures.....vii
List of Symbols and Abbreviations.....x
Acknowledgements.....xiii

Chapter 1 General Introduction.....1

1.1 Introduction.....2
1.2 Light-Emitting Devices: Historical Perspective.....2
1.3 Organic Light-Emitting Devices.....6
1.4 Polymer Light-Emitting Devices.....9
1.4.1 PPV and it's derivatives.....11
1.5 Problems with OLEDs and PLEDs.....13
1.6 Encapsulation of PPV.....16
1.7 Porous Alumina.....18
1.8 Goals of Thesis.....21

Chapter 2 Incorporation of Luminescent Polymers into Porous Alumina.....23

2.1 Introduction.....24
2.2 Experimental.....24
2.2.1 General.....24
2.2.2 Evaporation of Al Films on Si wafers.....25
2.2.3 Anodization of Al films.....26
2.2.4 Incorporation of Polymers into Porous Alumina films on Si and Al Substrates.....27
2.3 Results and Discussion.....28
2.3.1 Deposition of Al Films on Si and ITO Substrates.....28
2.3.2 Anodization of Al Films.....30
2.3.3 Polymer Incorporation into Porous Alumina Films.....32
2.3.4 Proposed Mechanism of Polymer Incorporation to Porous Alumina Films.....36
2.3.5 Attempt to Increase Polymer Loading.....38
2.4 Summary and Future Work.....38

Chapter 3 Investigations into the Nature of the Interaction between Polymer and the Pore Walls.....40

3.1 Introduction.....41
3.2 Experimental.....42
3.2.1 General.....42
3.2.2 Attempted Extraction of MEH-PPV adsorbed to Anodisc

Membrane....43
3.2.3 UV-vis Spectroscopy of MEH-PPV adsorbed to Anodisc Membrane....43
3.2.4 Silanization of Anodisc Membranes....44
3.3 Results and Discussion....44
3.3.1 Porous Alumina....44
3.3.2 Degree of Polymer Adsorption....45
3.3.3 Effect of Light and Air on Polymer Adsorbed to the Anodisc Membrane....48
3.3.4 Polymer-Pore Wall Interactions....50
3.4 Conclusions and Future Work....62

Chapter 4: Summary and Future Work....64

References....67

List of Schemes

Scheme 1.0.....12

Scheme 1.1.....12

Scheme 1.2.....14

Scheme 3.0.....51

List of Figures

Figure 1.0 Formation of bands from discrete energy levels in atoms and molecules in extended materials)..... 3

Figure 1.1 Band diagrams showing the difference between insulators, semiconductors, and metals..... 4

Figure 1.2 Band diagrams for p-type and n-type semiconductors showing effect of doping.....5

Figure 1.3 Historical development of LEDs.....7

Figure 1.4 Charge injection from cathode and anode resulting in electroluminscence.... 8

Figure 1.5 Energy diagrams for devices (a) without an ECHB and (b) with an ECHB...11

Figure 1.6 Energy diagrams illustrating a possible quenching mechanism in PPV via the intermediate between two model compounds.....16

Figure 1.7 Glass/epoxy device encapsulation under nitrogen.....17

Figure 1.8 Encapsulation of device using PPX/PCPX.....18

Figure 1.9 Formation of the pores from aluminium during the electrochemical process, (a) migration of Al^{3+} and O^{2-} to form Al_2O_3 (b,c) pore formation occurs at cracks and defects.....21

Figure 1.10 Schematic of polymer strands adsorbed to porous alumina.....22

Figure 2.0 Schematic of anodization cell.....27

Figure 2.1 SEM images of anodized Al on ITO substrates (not etched with H_3PO_4). Light areas on the surface may be regions where anodization is incomplete.....29

Figure 2.2 SEM images of porous alumina films (a) pores after a 'one step"anodization process on a Si substrate and (b) pores after a "two step"anodization process on aluminum foil,.....30

Figure 2.3 SEM images of cross-sectional view of porous alumina on (a) a porous alumina film on Al substrate with an alumina barrier layer of ~30 nm and (b) porous alumina films on Si, showing pores etched down to the Si substrate.31

Figure 2.4 SEM images of porous alumina on Si substrate (a) before polymer incorporation and (b) after polymer incorporation.....33

Figure 2.5 Cross-sectional view of porous alumina containing MEH-PPV under (a) visible and (b) UV light,.....34

Figure 2.6 Fluorescence micrographs at 50 x magnification of (a)MEH-PPV (b) DP-PPV (c)DP_{10}-PPV in porous alumina on Si. The white areas indicate regions of fluorescence.....35

Figure 2.7 Bronsted and Lewis acid sites on the pore walls of alumina.....37

Figure 2.8 Bonding between Lewis acid sites on porous alumina and Lewis basic sites on MEH-PPV.....37

Figure 3.0 Schematic for the silanization of pores.....41

Figure 3.1 SEM images of pores on Anodisc membranes.....45

Figure 3.2 UV-vis spectra of freshly prepared MEH-PPV and MEH-PPV recovered from Anodisc membrane in THF.....47

Figure 3.3 Normalized plot of λ_{max} of UV-Vis absorbance over time under conditions of light, dark , air and nitrogen.....49

Figure 3.4 Possible bonding modes with mono-, di-, or trichlorosilanes with alumina surfaces.....52

Figure 3.5 Surface morphology of a silane monolayer.....53

Figure 3.6 Surface reflectance IR spectra of (a) non-silanized, (b) TMS, (c) PDMS and (d) ODMS silanized porous alumina on Si at a grazing angle of 30 °. Arrows indicate a new band at 1260 cm^{-1}.....54

Figure 3.7 Si (2p) region of XPS spectra for (a) TMS, (b) PDMS and (c) ODMS silanized Anodisc membranes.....56

Figure 3.8 SEM images of (a) non-silanized and (b) TMS silanized porous alumina on Si.....57

Figure 3.9 SEM images of TMS silanized porous alumina (a) without MEH-PPV and (b) with MEH-PPV.....57

Figure 3.10 UV-vis Spectra of non-silanized and TMS, ODMS, and PDMS silanized Anodisc membranes with MEH-PPV.....58

Figure 3.11 Fluorescence spectra of non-silanized and TMS, PDMS, and ODMS silanized Anodisc membranes with MEH-PPV.....61

Figure 3.12 Fluorescence specctra of non-silanized and TMS, ODMS and PDMS silanized Anodisc membranes with DP_{10}-PPV.....62

List of Symbols and Abbreviations

Symbol	Description
Al_2O_3	alumina
Alq_3	8-tris-hydroxyquinoline aluminum
CCD	charge-coupled device
cd	candela
cm	centimetre
CVD	chemical vapour deposition
°C	degrees Celcius
DH-PPV	2,5-dihexyloxy poly(phenylene vinylene)
DP-PPV	2,3-diphenyl poly(phenylene vinylene)
DP_{10}-PPV	2,3-diphenyl–5-decyl poly(phenylene vinylene)
DSB	distyrylbenzene
e^-	electron
E_F	energy of Fermi level
eV	electron volt
ECHB	electron conducting/ hole blocking
EL	electroluminescence
FTIR	Fourier Transform Infrared
g	gram
hr	hour
HOMO	highest unoccupied molecular orbital
IR	infrared

ITO	indium tin oxide
LED	light-emitting device
LPE	liquid phase epitaxy
LUMO	lowest unoccupied molecular orbitals
M	molar
m^2	meters squared
mg	milligrams
min	minute
mL	millilitres
mTorr	millimetre Torr
μm	micron
nm	nanometer
ODMS	octyldimethylchlorosilane
OLED	organic light emitting device
p	para
p-n	p-type n-type semiconductor junction
PCPX	poly-2-chloro-*p*-xylylene
PEO	polyethylene oxide
PDMS	phenyldimethylchlorosilane
PL	photoluminescence
PLED	polymer light emitting device
PPV	poly(phenylene vinylene)
PPX	poly-*p*-xylylene

PVK	poly(9-vinyl carbozole)
ROMP	ring-opening metathesis polymerization
SEM	scanning electron microscope
SDA	stillbene-4,4'-dicarboxaldehyde
Sq	square centimetre
THF	tetrahydrofuran
TMS	trimethylchlorosilane
UV	ultraviolet
V	Volt
Vis	visible
w/w	percent by weight
W	Watts
XPS	X-ray photoelectron spectroscopy
∞	infinity
π	pi bonding orbitals
π^*	pi anti-bonding orbitals
Ω	Ohm
%	percent
ν	frequency (wavenumber)
λ	wavelength
λ_{max}	wavelength at maximum absorbance
λ_{ext}	excitation wavelength

Acknowledgments

I would like to thank my supervisor, Dr. M. O. Wolf for all his guidance and support. As well, all the members of the Wolf group who have made my stay at UBC unforgettable. I would especially like to thank Dr. Katja Rademacher who helped me on this thesis.

There are many people who lent their support in helping me. I would like to thank Dr. Alina Kulpa, Dr. Ken Wong, Dr. Ian Clark-Lewis, Dr. Dan Bizzottto, and Jeff Shephard. The mechanical shop at UBC has helped me greatly and I thank them for their time and patience.

I am very grateful to all my friends and family for lending they're ears for many many hours and for they're support, especially Tracey Stott.

Chapter 1

General Introduction

1.1 Introduction

In 1962, Holonyak developed the first commercially available light-emitting device (LED) based on GaAs.[1] Since this discovery, LEDs have found applications ranging from status indicators to flat-panel displays. These materials have created a multi-billion dollar industry, fuelling the search for better light-emitting materials. Applications such as traffic lights, which traditionally have used filtered incandescent lamps are gradually being replaced with these inorganic-based LEDs.[1] This change is predicted to save as much as $1000 per intersection per year due to the higher luminance efficiency and lower power consumption of LEDs. The development of inorganic-based LEDs has resulted in devices that are now comparable to the luminescence efficiencies of filtered fluorescent lamps.[2]

The development of LED technology has not been limited to inorganic materials. Over the past decade, organic and polymeric materials have emerged as candidates for LEDs. The success and rapid development of these materials have attracted the attention of such companies[1,3] as Philips, Uniax and Pioneer; however, commercialization of devices based on these materials requires improvements in performance. Issues such as tolerance of temperature and humidity variations as well as the operating lifetime of these devices are significant for commercialization.[4]

1.2 Light-Emitting Devices: Historical Perspective

A thorough understanding of how LEDs operate relies on band theory,[5] and a brief overview is given here. In small molecules, molecular orbitals consist of discrete energy levels. However, in extended materials where bonding exists between many

atoms, closely spaced energy levels exist. These bands, which exist over a range of energies, can be filled or empty. One arrangement consists of a filled band known as the valence band, corresponding to the HOMO in molecular terms, and a higher energy empty band, known as the conduction band (the LUMO in molecular terms) (Figure 1.0).

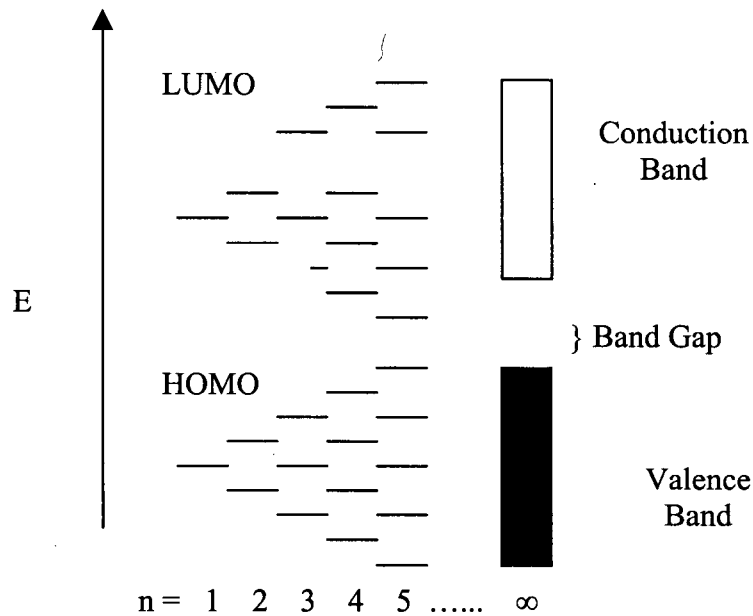

Figure 1.0. Formation of bands in extended materials from discrete energy levels in atoms and molecules.

The energy of the band gap (difference between the top of the valence and bottom of the conduction bands) determines if a material behaves as a metal (no gap), semiconductor (small gap) or insulator (large gap) (Figure 1.1).

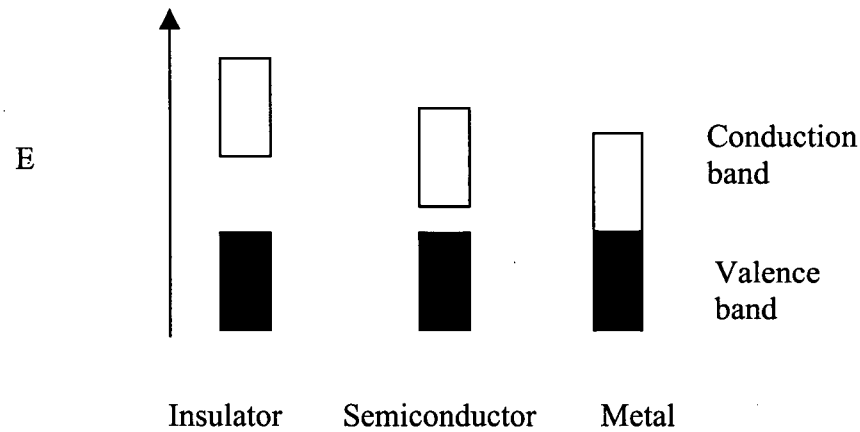

Figure 1.1. Band diagrams for insulators, semiconductors and metals.

In semiconductors, discrete energy levels can be introduced in the band gap through doping, or adding a small amount of an impurity to the pure material. When doped with an element that has less valence electrons than the semiconductor, empty discrete energy levels are formed in the band gap near the top of the valence band, known as acceptor levels. The energy difference between the valence band and the acceptor levels is typically on the order of 0.1 eV. This gap is small enough that electrons in the valence band can thermally populate the acceptor levels, creating positive "holes" in the valence band. Such a material is known as a p-type semiconductor.

On the other hand, if the semiconductor is doped with an element that has more valence electrons, filled discrete energy levels are formed near the bottom of the conduction band, known as donor levels. The energy difference between the donor levels and conduction band is also small, allowing for electrons to populate the empty conduction band thermally. This adds negative charges to the conduction band and results in n-type doping (Figure 1.2).

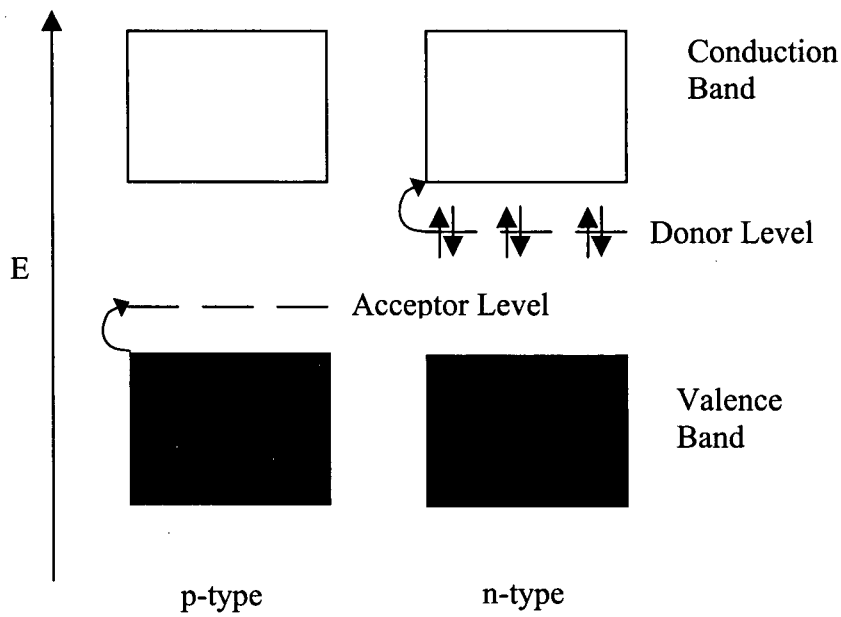

Figure 1.2. Band diagrams for p-type and n-type semiconductors, showing effects of doping.

Conventional LEDs are composed of a p-i-n junction.[1,6] Under an applied potential, injected charges migrate towards each other and recombine at the p-n interface resulting in light emission. This process of converting electrical current to light is known as electroluminescence (EL). In inorganic LEDs, semiconductors such as GaAs which emit light efficiently are used. Modifications such as doping of GaAs with other elements such as Al or P have led to devices with different colours. For many years, inorganic LEDs were limited to indoor applications as their brightness was insufficient for outdoor usage or bright sunlight applications. Adjustments to the amount and type of dopant used resulted in improvements to the luminescence efficiencies. The first commercial inorganic LED was GaAsP and since then many different doped inorganic materials have been used such as InGaN and AlGaInP.[6]

Inorganic LEDs are made by deposition of a thin film of the semiconductor by sputtering, chemical vapour deposition (CVD) or liquid phase epitaxy (LPE).[6] As well, the thin films must be grown on a substrate that has a matching lattice otherwise small defects created from the lattice mismatch result in the formation of non-radiative sites. As many of the inorganic materials are GaAs based, this is the most common substrate. However, it has been found that GaAs reabsorbs most of the light emitted towards it, lowering the luminescence efficiency. To eliminate this, a transparent substrate such as GaP may be used, however the lattice match is not as good as with GaAs.[6] The development of inorganic-based LEDs has taken many decades and improvements are still being made to commerical devices.

1.3 Organic Light-Emitting Devices

A new route to electroluminescent devices, which has been developed over the last decade, uses organic emitters. It has been known for many years that some organic materials, such as anthracene,[7] have high photoluminescence quantum yields and could therefore be useful in LEDs. High turn-on voltages, however, have hindered devices based on these materials from becoming commercially viable. Studies toward improved organic materials have been quite promising and some of the performance parameters of these materials now match those of their inorganic counterparts (Figure 1.3).[8]

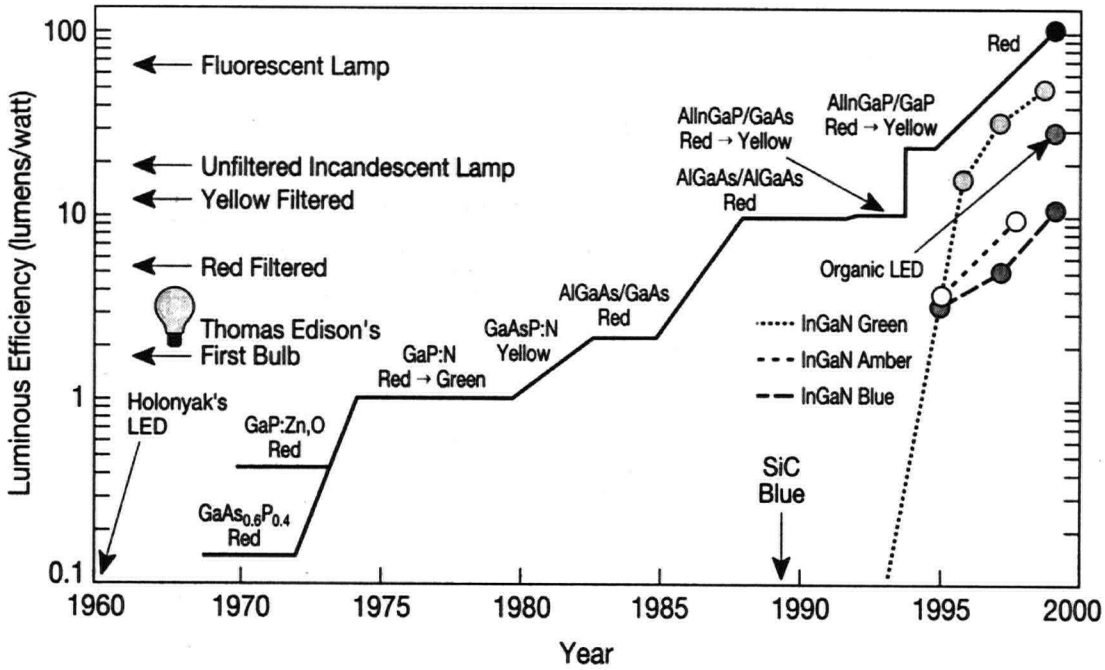

Figure 1.3. Historical development of LEDs (used with permission).[1]

The design of a basic organic light-emitting device (OLED) is similar to that used in currently available inorganic devices. Two electrodes, one of which is transparent are used, and the organic material is sandwiched between the electrodes. Under an applied potential, electrons are injected into the HOMO (or valence band) of the emitter at the anode and the LUMO (or conduction band) at the cathode (Figure 1.4).

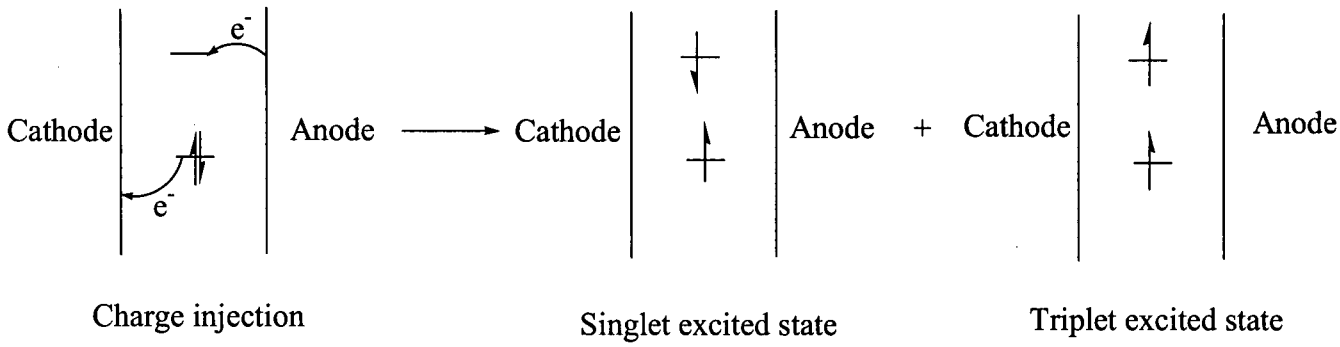

Figure 1.4. Charge injection from the cathode and anode, resulting in electroluminescence.

The injected charges migrate towards each other in the organic layer, and eventually recombine resulting in the emission of light. In 1987, Tang *et al.*[3,7,8] fabricated one of the first OLEDs with a luminance of over 1000 cd m^{-2}. This luminance is sufficient for many applications and was observed at an operating voltage below 10 V. In this two-layer device, N,N'-diphenyl-N,N'-bis(3-methylphenyl)-[1,1'-biphenyl],-4,4'-diamine **(1)** and 8-tris-hydroxyquinoline aluminum (Alq_3) **(2)**, were sequentially sublimed onto a magnesium-silver cathode.[3]

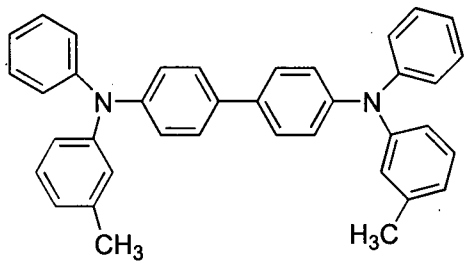

1

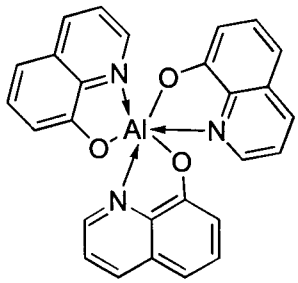

2

Transparent indium tin oxide (ITO) was used as the anode. In this device, hole-injection occurred at the ITO electrode, the triarylamine acts as a hole-transporting layer, and the Alq_3 is the electron-transporting layer and emitter. The magnesium-silver alloy acts as the election-injecting electrode. Small organic molecules, such as Alq_3, are still under development as emitters and some of the first commercially available OLEDs such as those sold by Pioneer are based on this material.[3]

1.4 Polymer Light-Emitting Devices

The demonstration of high luminance efficiencies in OLEDs has stimulated much research toward better organic devices. Improvements to the device fabrication used by Tang *et al.* were possible since these OLED devices require sublimation to deposit the organic material as a thin film. In 1991, Friend *et al.*[3,4] in Cambridge discovered that the conjugated polymer poly (phenylene vinylene) (PPV) **(3)** could be used as an emitter in an electroluminescent device. This discovery suggested a wide variety of possible opportunities for improvement to OLEDs.

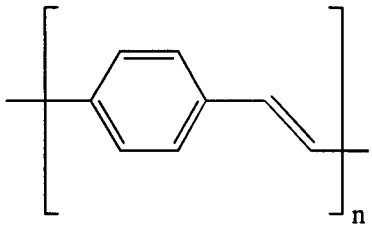

3

Some of the advantages offered by polymers are that they may be synthesized easily, are relatively cheap and are flexible, allowing for new device architectures that were not possible with brittle inorganic materials. In general, polymer light emitting devices

(PLEDs) have the same basic structure as devices based on small molecule organic materials, with two electrodes (one with a high work function and one with a low work function) and the polymer layer sandwiched in between them. The EL quantum yield of OLEDs and PLEDs is believed by many researchers in the field to have an upper limit of 25% of the PL quantum yield of the emitting material.[9,10,11] This is a consequence of the fact that only 25% of charge carriers with uncorrelated spins can recombine to give emissive singlet excited states. However, the effects of magnetic fields and intermolecular effects such as excimer emission or extrinsic quenching on PL quantum yield are not yet completely understood.

It has been found that organic polymers such as PPV are better at transporting holes than electrons as they typically have low electron affinities.[2,12] This results in unbalanced charge injection into these materials, and consequently in recombination of charges near the metallic cathode, which may quench the exciton. One way to overcome this problem is to introduce an electron-conducting, hole-blocking (ECHB) layer between the cathode and the emitter layer, (Figure 1.5). The ECHB must have a valence band lower in energy than that of the emitter and have an electron affinity the same or greater in energy than that of the emitting layer. This will result in the confinement of the holes at the emitting layer/ ECHB interface, leading to lower exciton recombination near the electrode.

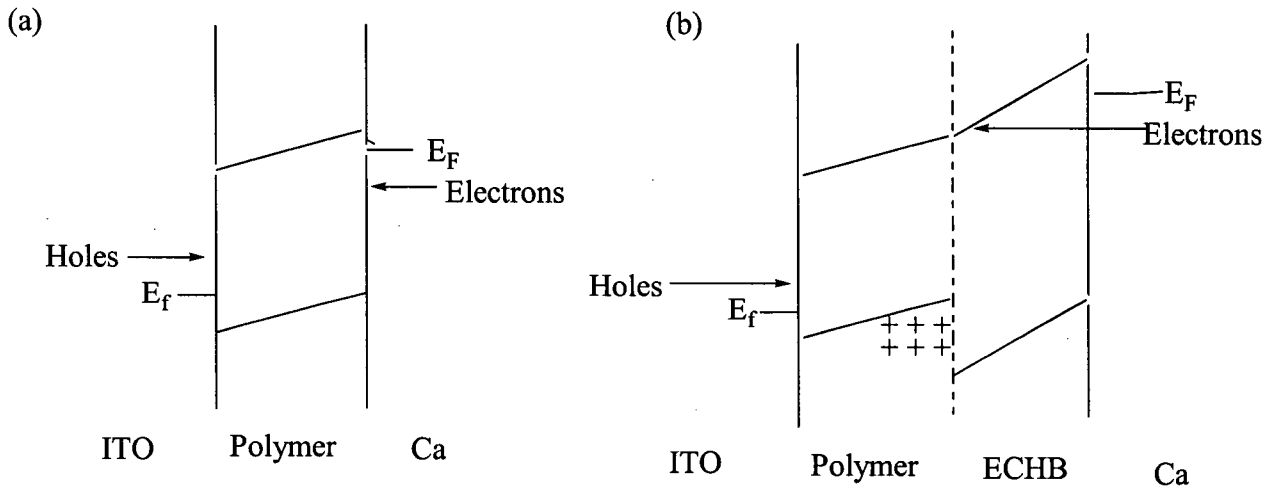

Figure 1.5. Energy diagrams for devices (a) without ECHB and (b) with an ECHB.

1.4.1 PPV and its Derivatives

Subsequent to the discovery that PPV could be used in electroluminescent devices, this polymer received a lot of attention. PPV is photoluminescent, emitting in the visible, with a yellowish colour resulting from the π^* to π transition of approximately 2.5 eV.[13]

PPV is a rigid-rod polymer that is thermally stable, and can withstand elevated temperatures sometimes encountered during device operation. The polymer can be synthesized by a variety of methods, with the most common route involving the synthesis of a soluble sulfonium precursor polymer followed by thermal treatment to convert this to insoluble PPV (Scheme 1.0). PPV has also been synthesized by CVD,[13] electrochemical methods[14] and by chemical[2,13] routes using the Wittig and Heck reactions, and ring opening metathesis polymerization (ROMP).[13] Another common route to PPV is via the Gilch[13,15] route that involves dehydrochlorination with potassium *tert*-butoxide (Scheme

1.1). These various route result in different polymer molecular weights, which can affect the luminescence behaviour of the polymer.

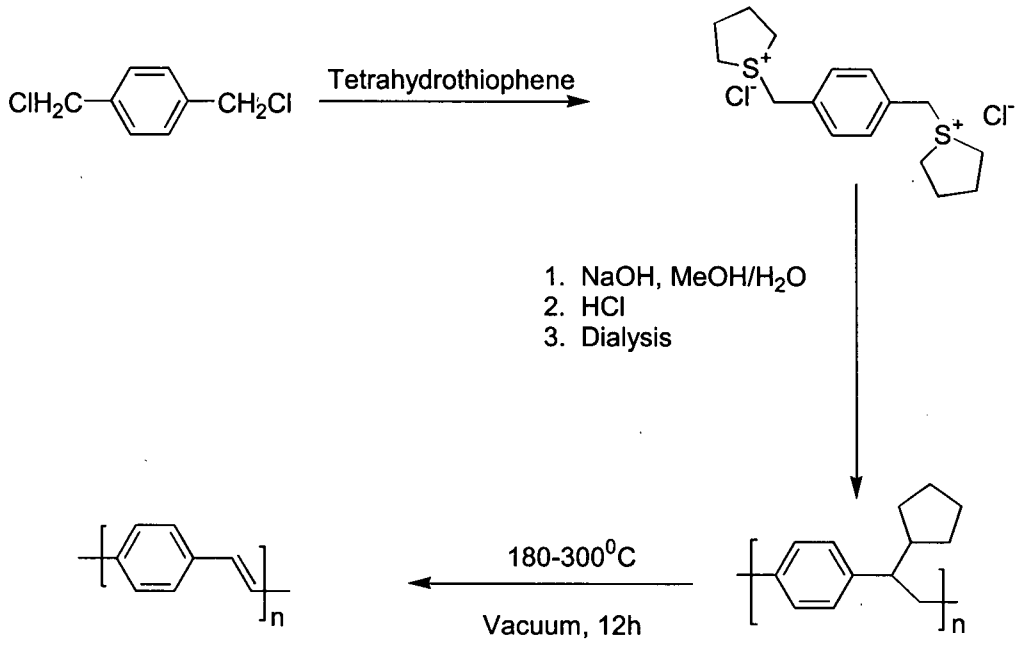

Scheme 1.0

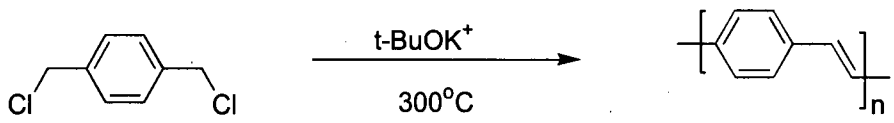

Scheme 1.1

Although PPV was used in the first PLED, this material is not optimal for a number of reasons. Principally, the insolubility of PPV complicates device fabrication. To increase the solubility and therefore processibility of PPV in organic solvents, side-chains have been added to the polymer backbone. In 1989, Wudl *et al.*[2] were the first to synthesize a soluble PPV derivative, a dihexyloxy-substituted poly(phenylene vinylene)

(DH-PPV) **(4)**. This polymer is soluble in organic solvents such as THF and chlorobenzene above 80 °C.[2,13] The potential advantages of a polymer which is soluble at room temperature led to a search for such a material, resulting in the discovery of an asymmetrical dialkoxy substituted polymer, poly-((2-methoxy-5-(2'ethylhexoxy) phenylene vinylene) (MEH-PPV) **(5)**. As a consequence of its superior solubility, many studies have focused on this polymer which has a band gap of 2.2 eV[13] and emits orange-red light. Devices based on alkoxy derivatized PPVs have been shown to have operating voltages below 2 V with a luminance of 100 cd/m^2 at 2.4 V. This is similar to the brightness of a colour TV.[8] Since the discovery of MEH-PPV, other soluble substituted-PPV polymers have also been prepared and studied. PLEDs are very promising and are expected to play a major role in the development of second-generation light emitting devices.

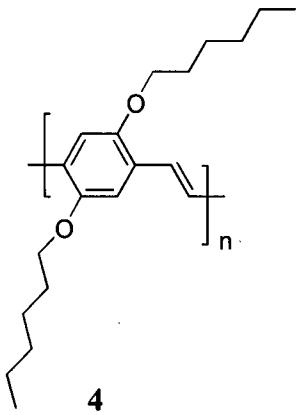

4

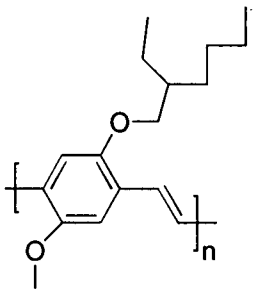

5

1.5 Problems with OLEDs and PLEDs

Some of the difficulties that have hindered the widespread commercial introduction of OLEDs are also significant in PLEDs. In both cases, device stability on the shelf, as well as during operation, and decreases in luminance efficiency during

operation are a concern. In both OLEDs and PLEDs, black spot formation has been observed in devices after operation. It is believed to be the result of degradation of the organic or polymeric material.[16] For OLEDs based on Alq_3, the emitter has been known to react with water in the air to form 8-hydroxyquinoline (Scheme 1.2),[17] which reacts with oxygen to form a dark non-emissive polymer. In EL polymers two phenomena which cause decreases in light output are interchain interactions and degradation due to oxidation of the polymer.[9,18,19,20]

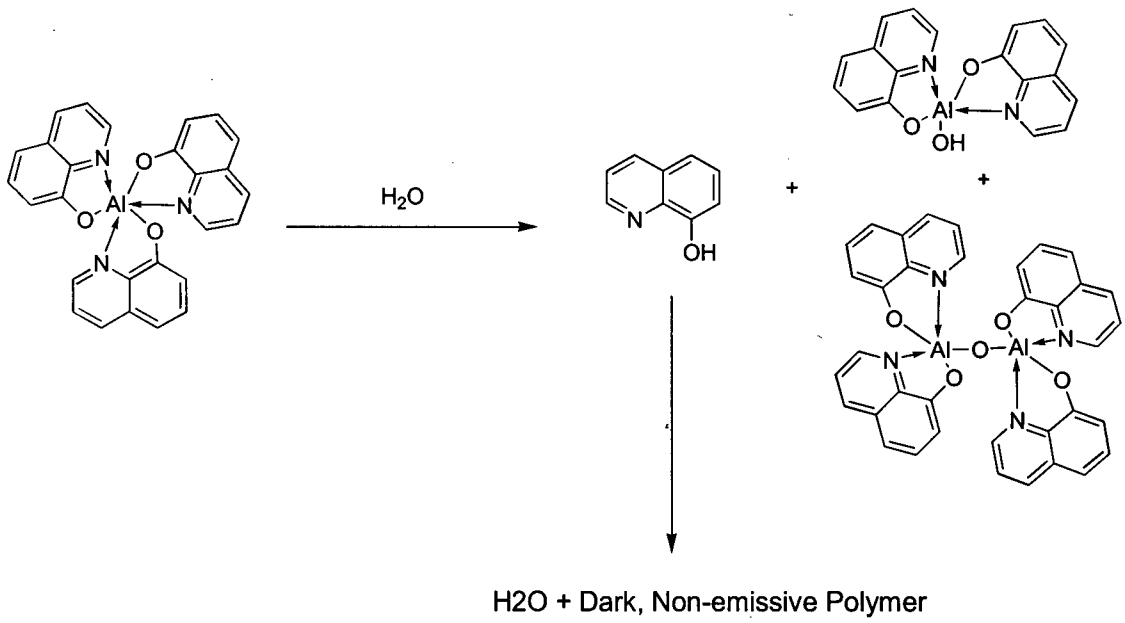

Scheme 1.2

In conjugated polymers, charge may be carried both along the π-backbone as well as between chains via interchain interactions, such as π-stacking. The PL of thin MEH-PPV films, dilute solutions and a blend of MEH-PPV and polystyrene films have been studied.[21] These studies showed that the PL intensity from MEH-PPV films was significantly lower than from dilute solution or polymer blend films.[21] The PL spectrum

of the thin film was believed to contain emission from spatially indirect excitons. These emissive excitons influence the PL intensity,[21] thus it is of interest to find methods of reducing the degree of interchain interaction in these materials.

The device lifetime is critical in determining the commercial viability of devices based on PPV-type polymers. The stability of a thin film of MEH-PPV on ITO in an inert atmosphere has been studied under irradiation with UV light. IR studies[11,20] revealed the formation of C-O stretching bands characteristic of an aromatic aldehyde along with a corresponding decrease in the intensity of the C=C stretching band, suggesting the C=C bonds in the polymer are being oxidized. Since these experiments were performed under nitrogen, the oxygen source is believed to be the ITO substrate. Adding a layer of doped polyaniline/polystyrenesulfonic acid on top of the ITO decreases the rate at which the PL intensity drops, suggesting that the presence of the polyaniline/polystyrenesulfonic acid prevents oxygen from the ITO from reacting with the PPV.[22]

The oxidation of the polymer results in a lowering of the luminescence efficiency due to quenching from the carbonyl groups. Rothberg *et al.*[9] have found that one carbonyl defect for every 400 phenylene vinylene units quenches the PL by as much as a factor of two. A model[9,11] of how this quenching occurs was carried out by studying the behaviour of shorter oligomers of PPV. *Trans*-stilbene-4,4'-dicarboxaldehyde (SDA) is highly luminescent, in contrast to photo-oxidized PPV. A model compound for PPV is 1,4-*trans, trans*-distyrylbenzene (DSB), which has slightly higher HOMO and LUMO energy levels than SDA. Since the difference in energy between SDA and DSB is very small, electron transfer between the two is favourable. This transfer of charge from DSB

to SDA results in quenching of the PL. This was also observed experimentally when films of mixtures of DSB and SDA were studied (Figure 1.6).

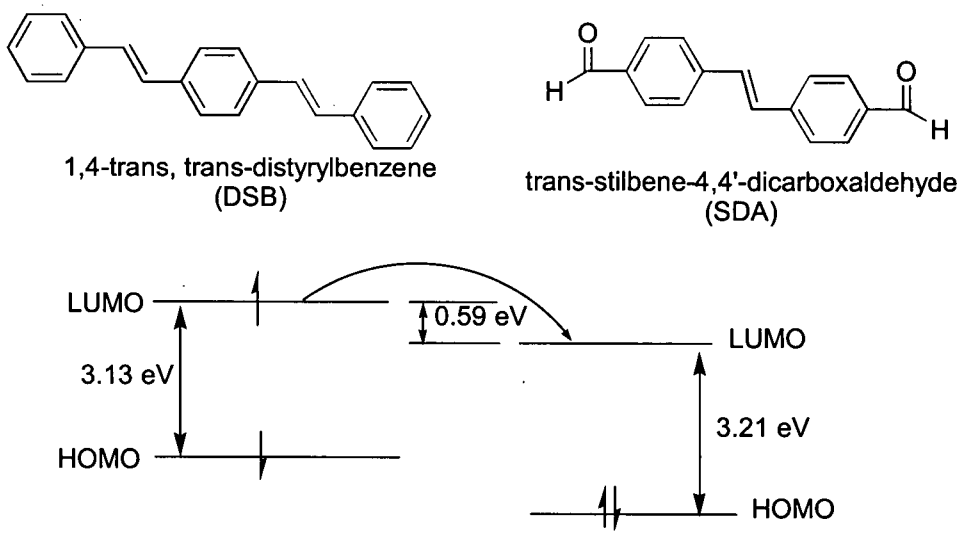

Figure 1.6 Energy diagrams illustrating a possible quenching mechanism in PPV.

1.6 Encapsulation of PPV

To address the problems encountered with the use of organic and polymeric materials as the emitting layers in EL devices, many routes to improve the luminescence efficiency have been explored. As mentioned earlier, one of the problems with polymeric materials is related to interchain interactions. Some approaches that have been investigated to avoid these including making modifications to the polymer structure,[23] adding bulky or bridging side groups to the polymer or the deliberate addition of *cis* double bonds to prevent close packing. Another approach is to make polymer blends to prevent aggregation.[21] To protect the emitting layer from oxidative degradation due to atmospheric oxygen or water, devices have been encapsulated in an inert atmosphere

such as nitrogen. For example, Burrows *et al.*[24] have encapsulated devices in an inert atmosphere with epoxy and glass (Figure 1.7).

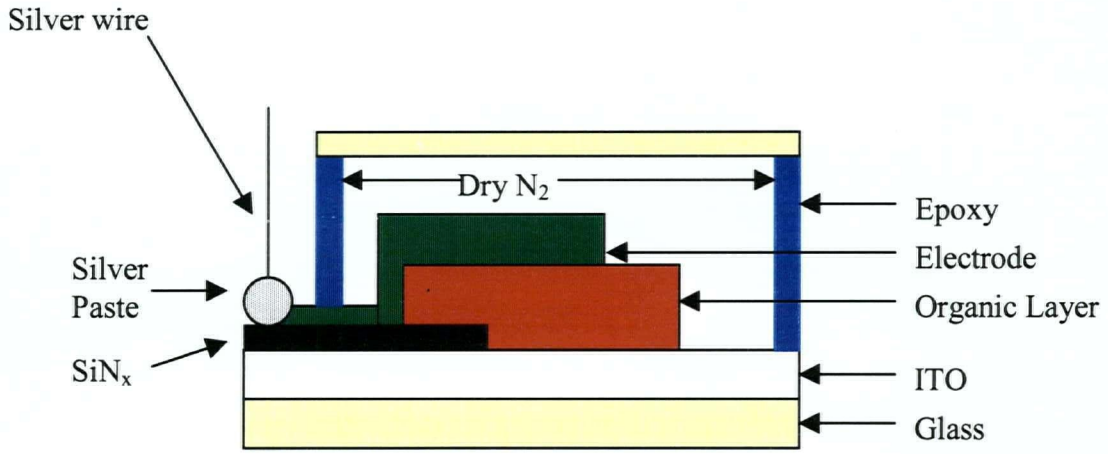

Figure 1.7 Glass/epoxy device encapsulation under nitrogen.

This approach increases the device thickness and the number of fabrication steps significantly. Yamashita *et al.*[25] have improved upon this encapsulation method by using chemical vapour deposition of thin films of poly-*p*-xylylene (PPX) and/or poly-2-chloro-*p*-xylylene (PCPX) (Figure 1.8), to decrease device thickness while still encapsulating the emitter layer. In both cases, the lifetime of the devices was found to be greater than for a non-encapsulated device.

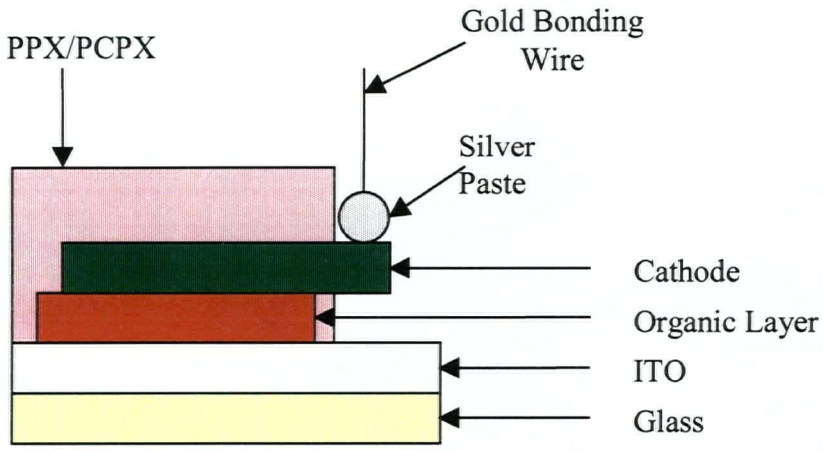

Figure 1.8 Encapsulation of a device using PPX/PCPX.

An alternative approach to improving the stability of the emitter is to encapsulate the organic material directly within a host matrix. This does not result in an increase in device thickness. The host-guest approach to encapsulation requires that the host material be chemically inert, have low absorbance in the visible region and be easy to fabricate. One material that satisfies all these criteria is porous alumina, a material that is formed by anodic etching of Al films.

1.7 Porous Alumina

Porous alumina, has been used for various applications ranging from in the dye industry for decorative purposes,[26] to corrosion resistance[27], to functioning as a template for nanotubes.[28] More recently, it has also attracted attention for its ability to behave as a photonic crystal[29] and as a possible material for use in information storage devices.[28,29]

In porous alumina, the pores are arranged in a hexagonal array, and are formed via an electrochemical process known as anodization.[30,31] The exact mechanism of pore

formation is not completely understood but it has been postulated that during this process several chemical reactions are occurring simultaneously.[30] Two of the principal reactions are the oxidation of Al to Al^{3+} and the formation of O^{2-} by water splitting.[30]

$$Al(s) \rightarrow Al^{3+} + 3e^- \quad (1)$$

$$3/2\ H_2O \rightarrow 3H^+ + 3/2\ O^{2-} \quad (2)$$

These ions react with one another to form a rough barrier layer of Al_2O_3 at the metal/electrolyte interface.[30,31] This results in cracks and defects at the surface, which are believed to act as sites for pore nucleation. The electric field that is generated is not uniform across this layer, but is higher at areas that have cracks and defects, as the barrier layer is thinner.[30] This allows for more ions to diffuse across the barrier layer to form more Al_2O_3 at the oxide/electrolyte and oxide/metal interface. There is no build up of this barrier layer in the cracks and defects because the alumina is slightly soluble in the electrolyte (eq.3).[26,30,31]

$$1/2Al_2O_3 + 3H^+ \rightarrow Al^{3+} + 3/2\ H_2O \quad (3)$$

Due to the increase in electric field, it is believed that local heating at the cracks and defects occurs, allowing for a higher solubility of Al_2O_3 in the electrolyte.[27] The formation of the hexagonal array is believed to be due to repulsive forces caused by mechanical stress (Figure 1.9).[32]

During this process, two parameters are very important. The first is the choice of electrolyte; which must be able to dissolve some of the barrier layer alumina. It has been found that phosphoric acid, sulfuric acid and oxalic acid are all good electrolytes. It has also been shown that H_3PO_4 forms larger pores whereas oxalic acid results in smaller

pores.[24] This may be due to the acidity of the electrolyte, as H^+ ions from the electrolyte are needed to form H_2 gas.[26]

$$3H^+ + 3e^- \rightarrow \frac{1}{2} H_2 (g) \quad (4)$$

The second parameter that is very important is the potential applied to the system. A higher applied potential gives a higher electric field, resulting in larger pores.[30] These two parameters should be considered together. The use of H_3PO_4 requires lower applied potentials to achieve pores with diameters of 200 nm or greater, whereas when oxalic acid is used, an applied potential of 40 V creates pores with diameters of 50-70 nm. To obtain the desired pore diameter, both the voltage and the electrolyte must be chosen carefully.

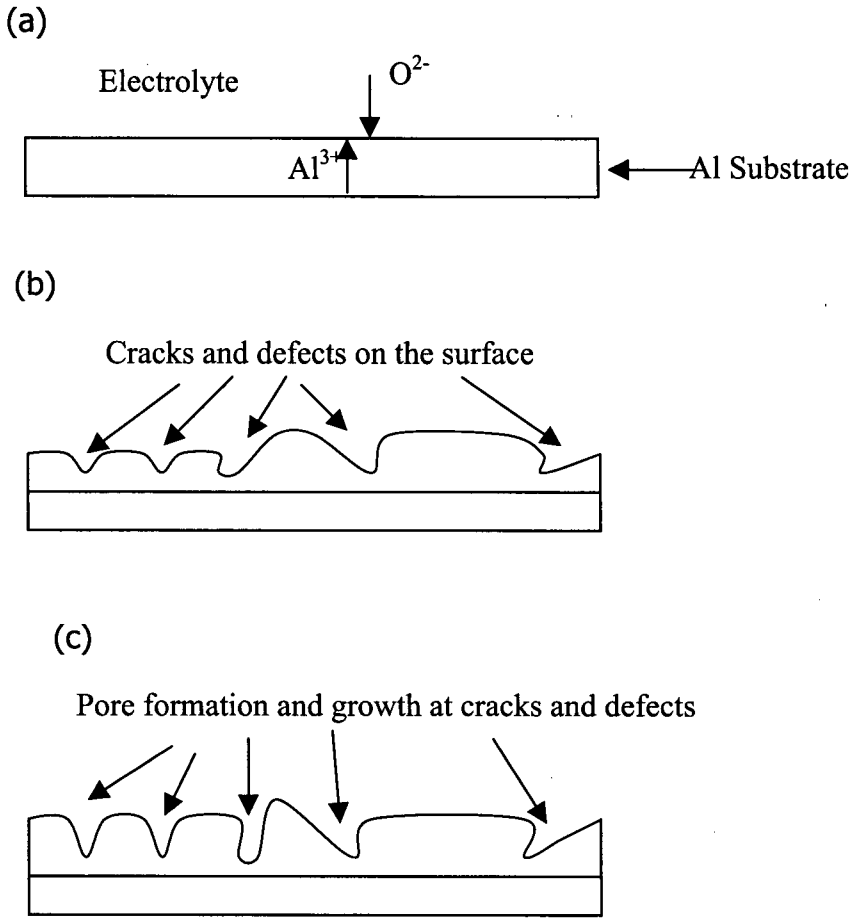

Figure 1.9 Formation of pores from aluminum during the electrochemical process, (a) migration of Al^{3+} and O^{2-} to form Al_2O_3, (b,c) pore formation and growth occurs at cracks and defects.

1.8 Goals of Thesis

Some of the major problems with using organic and polymeric materials in EL devices are due to oxidation effects and interchain interactions. A possible device design that would minimize or even possibly eliminate these problems would be to encapsulate the luminescent polymers into a nanoporous host such as porous alumina (Figure 1.10). A similar approach has been investigated by Gruzinskii *et al.* who incorporated coumarin-7 into porous alumina.[33] With sufficiently small pores, one polymer chain per

pore could be encapsulated thereby preventing polymer aggregation and eliminating interchain interactions. In addition, the host material could offer protection against atmospheric oxygen and water, thus slowing down degradation of the polymer.

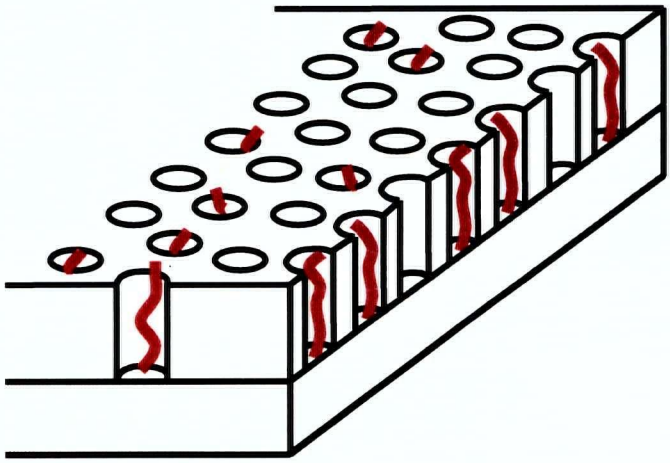

Figure 1.10 Schematic of polymer strands adsorbed to porous alumina.

The goals of the work in this thesis are to encapsulate the luminescent polymers MEH-PPV, DP-PPV, DP_{10}-PPV into a porous alumina host material. The effects of the chemical environment within the pores in which the polymer is located will be investigated by functionalizing the pore walls with a series of silanes. As well, degradation studies of MEH-PPV encapsulated in porous alumina will be carried out in order to probe the stability of the hybrid material.

Chapter 2

Incorporation of Luminescent Polymers into Porous Alumina Films

2.1 Introduction

Although organic polymers are believed to be viable candidates for the next generation of light-emitting devices, low luminescence efficiency and operational lifetimes have prevented these materials from reaching their full potential. As discussed in Section 1.5, these poor characteristics are related to interchain interactions and oxidative reactions in the polymer. Using directed synthesis of the polymer and careful device design, these problems have been minimized. However, much improvements can still be made. Encapsulation has been put forward as a possible strategy to minimize these undesirable effects. The approach that is explored in this thesis is the encapsulation of electroluminescent polymers in an ordered host material, porous alumina. Porous alumina is an ideal choice due to its ease of fabrication, chemical inertness and low absorbance in the visible region. Encapsulation is expected to result in the minimization of interchain interactions as well as alignment of the polymer relative to the electrodes. In addition, encapsulation in porous alumina may also offer protection of the polymer from oxidative degradation. In this chapter, the preparation of porous alumina and the incorporation of three luminescent polymers, MEH-PPV, DP-PPV and DP_{10}-PPV into this host will be described.

2.2 Experimental

2.2.1 General

All fine chemicals were purchased either from Aldrich, Fisher Scientific, Fluka or Acros and used as received. Aluminium sheet (99.99+%, 10 × 10 × 13 mm) was cut into small pieces (~1 cm × 1 cm) and used without further treatment. <100> n-type

(phosphorus doped) silicon wafers with a resistance between 5-8 Ω/sq. were purchased from Virginia Semiconductor Inc. Thermal evaporation of Al was carried out on a CHA Industries Thermal evaporator. Plasma etching was done on a Plasma Therm instrument. Indium tin oxide (ITO) glass slides (25 × 75 × 1.1 mm, 100 Ω/sq.) were purchased from Delta Technologies. MEH-PPV was synthesized by Dr. Katja Rademacher in our group. DP-PPV was synthesized following the procedure of Hsieh et *al.*[34] A sample of DP_{10}-PPV was kindly donated by Dr. Bing Hsieh of Canon Inc., and used without further purification. SEM images were obtained on a Hitachi S-4100 field emission microscope, using the Quatro Pro imaging program. Fluorescence microscopy was carried out on an Olympus IX70 microscopy using a real time CCD to capture the image. The microscope was calibrated using gratings supplied by Olympus.

2.2.2 Evaporation of Al Films on Si Wafers

Prior to Al deposition, the *n*-type Si wafers were treated with a 10% w/w HF solution to remove any silicon oxide and dried under N_2. The wafers were then immediately transferred to the evaporator. The Al was thermally evaporated at a base pressure of 10^{-6} torr. The thickness of the Al layer was determined by a thickness monitor in the chamber. To deposit approximately 1 μm of Al, the evaporator had to be loaded twice, and the film was therefore exposed to air during the reloading of Al.

Prior to evaporation of the Al films, the ITO substrates were thoroughly cleaned first by sequential sonication in a solution of cetyltrimethylammonium chloride, ethanol, acetone and then distilled water. This was followed by treatment with an oxygen plasma using an O_2 flow rate of 200 cm^3/min, pressure of 500 mTorr and a power of 200 W for

15 minutes. This allowed for removal of any residual carbon from the surface. Al films were then evaporated as described for the Al deposition on Si wafers. The resulting Al layer was approximately 1 μm in thickness.

2.2.3 Anodization of Al Films

The anodization cell used to prepare the porous alumina films is depicted in Figure 2.0 and was designed by Mr. Andras Pattantyus-Abraham in our group and built in-house by the UBC machine shop. A platinum mesh or wire is used as the cathode and the electrolyte was 0.3 M oxalic acid. Anodization was carried out with an applied voltage of 40 V, and the electrolyte solution was stirred throughout. The steady state current was typically 5.0 mA during anodization and a drop in current typically occurred after approximately 10 minutes of anodization. The applied voltage was turned off after the steady state current dropped to approximately 1.5 mA. The sample was then removed from the cell, washed with distilled water and placed in a vial containing a 5% w/w solution of phosphoric acid for 45 minutes. The sample was then washed first with distilled water, then with ethanol and finally dried under N_2.

The anodization procedure used for the Al films on ITO substrates was identical, with the exception that a sudden increase in current to approximately 20 mA occurred after 10 min. The applied voltage was turned off after this increase occurred. These samples were not etched with 5% w/w phosphoric acid.

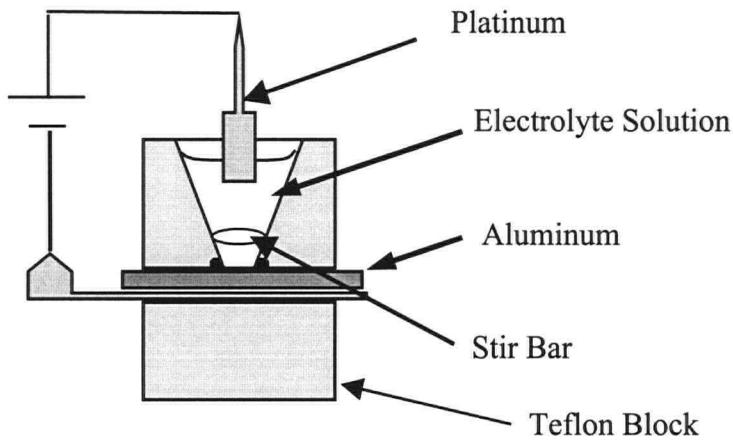

Figure 2.0 Schematic of anodization cell.

An alternative preparation involved using Al foil as a substrate. The foil was hand pressed between two glass slides to obtain a relatively flat surface, and then washed with ethanol and acetone to remove soluble organics. The anodization procedure used was identical to that used for anodizing Al on Si substrates with the following changes: the anodization was stopped after one hour, and at this point the current did not significantly differ from that measured when the anodization process was started.

2.2.4 Incorporation of Polymers into Porous Alumina Films on Si and on Al Substrates

The substrates were first placed under vacuum (approximately 0.5 mm Hg) for one day to remove any residual water or oxygen from the pores. The films were then immersed in a 0.03% w/w solution of MEH-PPV, DP-PPV or DP_{10}-PPV in THF for two days at room temperature in the dark. After two days, the films were removed and

immersed in a vial containing THF to remove polymer which was not adsorbed. This rinse was repeated four times with fresh THF until no further colour was extracted from the films. The samples were then dried under nitrogen in the dark.

DP-PPV was incorporated into the porous alumina films on Si and Al substrates according to the procedure described above, with the following changes: after incorporating the polymer and drying the sample under N_2 in the dark, the hybrid films were transferred to a Schlenk flask and placed under vacuum. The sample was then heated to 280 °C for two hours.

2.3 Results and Discussion

2.3.1 Deposition of Al Films on Si and ITO Substrates

The preparation of the nanoporous alumina films was carried out via an electrochemical process originally developed by Keller *et al.*[27] Using this method, it is possible to prepare porous alumina films on a variety of different substrates. The simplest method is to use Al foil as a substrate in which the thickness of the alumina layer can be varied. Thin films of porous alumina can also be prepared by anodization of evaporated Al films on other substrates. In this work, two substrates that are of particular interest are silicon and ITO as these materials are able to act as electrodes for charge injection in electroluminescent devices.

The thermal evaporator used in this work was able to deposit approximately 500 nm of Al at a time. In order to deposit a 1 μm film, the evaporator had to be opened to the atmosphere to allow reloading of the Al source. In doing so, the initially deposited Al film is likely covered with a thin oxide layer, possibly influencing the adhesion of the

second Al deposition. However, reloading of the Al source does not appear to interfere with the anodization process. For deposition on Si substrates, the Al layer adheres well to the Si and the film does not peel off during anodization. On the ITO substrates, adhesion was not as good despite careful cleaning of the ITO substrate before Al deposition. Cleaning the ITO with an O_2 plasma resulted in improved Al adhesion but anodization resulted in some peeling of the film from the substrate as well as some areas in which oxidation of the aluminium appears incomplete. SEM images (Figure 2.1), of areas of these samples in which the alumina film is adhered show pores are present, although not hexagonally ordered as has been achieved on Al substrates. The phosphoric acid etch was not carried out on these films due to the fragility of the layer.

One approach which may improve adhesion is to heat the ITO surface prior to deposition to remove any residual moisture, as well as after deposition in order to anneal the surfaces. This was not possible with the thermal evaporator used in this work as there is no heating stage. Due to these adhesion difficulties, further experiments with Al on ITO were not pursued.

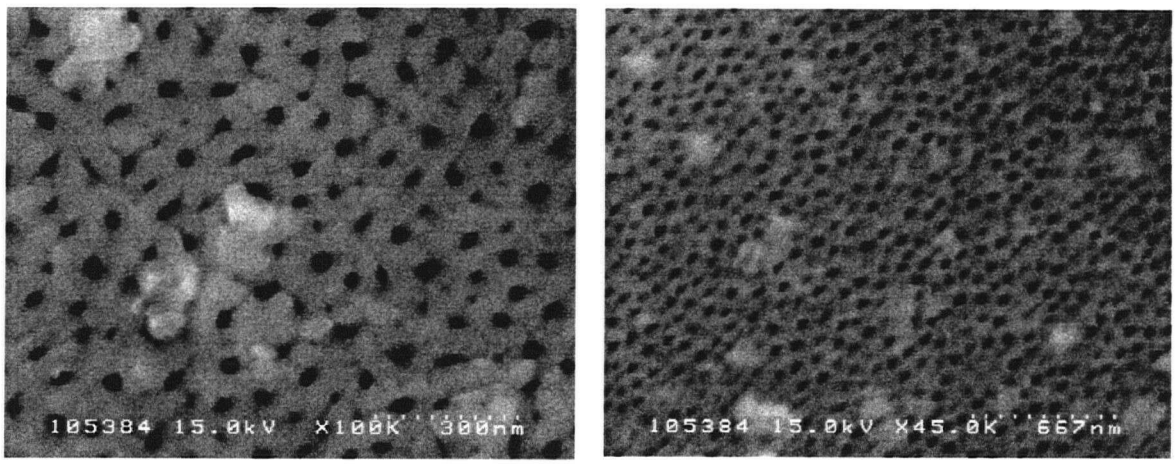

Figure 2.1 SEM images of anodized Al on ITO substrates (not etched with H_3PO_4). Light areas on the surface may be regions where anodization is incomplete.

2.3.2 Anodization of Al Films

The process used to generate the porous alumina films involved anodizing the Al films at 40 V in 0.3 M oxalic acid. These were found to be the optimal conditions to obtain pores ranging in size from 50-70 nm.[29,32,35] On a molecular scale, these are relatively large pores and are therefore expected to contain more than one polymer chain per pore, however, smaller pores are significantly more difficult to obtain[36] and so we elected to use the 50-70 nm pores for initial studies of polymer incorporation. After one anodization of an Al substrate, the pores are not arranged in a perfectly hexagonal array but are somewhat disordered (Figure 2.2a). To achieve well hexagonally-ordered pores, a second anodization is required after removal of the first porous alumina film with a solution of mercury(II) chloride (Figure 2.2b).[28] Such a "two-step" anodization process was not possible on the Al thin films on Si and ITO due to the limited thickness of the Al. The impact of the degree of pore ordering on the properties of the hybrid materials is not known at this point and was not pursued further.

(a) (b)

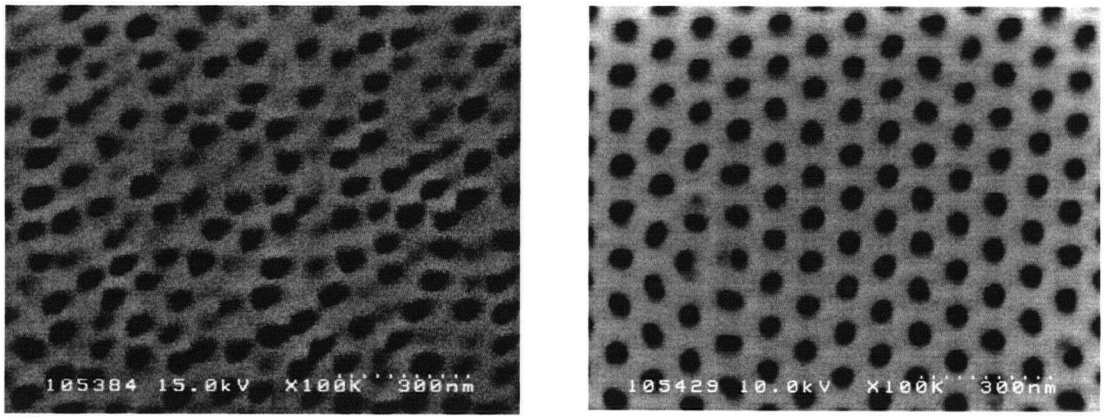

Figure 2.2 SEM images of porous alumina films (a) after a "one step" anodization process on a Si substrate and (b) after a "two step" anodization process on aluminum foil (images obtained by Dr. Katja Rademacher).

When silicon is used as a substrate, the level of Si doping is important. Crouse *et al.*[32] have reported that the use of *n*-type Si is better for anodization, since the process proceeds until the Si is exposed, whereas for *p*-type Si an unfavourable reaction occurs with the electrolyte solution. On *n*-type Si, a barrier layer with a void below remains after anodization, however, this is readily removed via etching with H_3PO_4. A SEM image of a cross-section of the porous alumina on Si film has been obtained (Figure 2.3). The cross-sections are obtained by cooling the sample in liquid nitrogen and then breaking the sample by hand, providing a clean edge with minimal damage to the porous alumina film. From these SEM images, the pores appear to be anodized all the way to the Si substrate. A cross-sectional view of porous alumina prepared on Al foil by Dr. Katja Rademacher in our group shows that there is a barrier layer at the bottom of the pores approximately 30 nm in thickness. This alumina barrier layer is insulating and therefore may hinder efficient charge injection into the hybrid layers.

(a) (b)

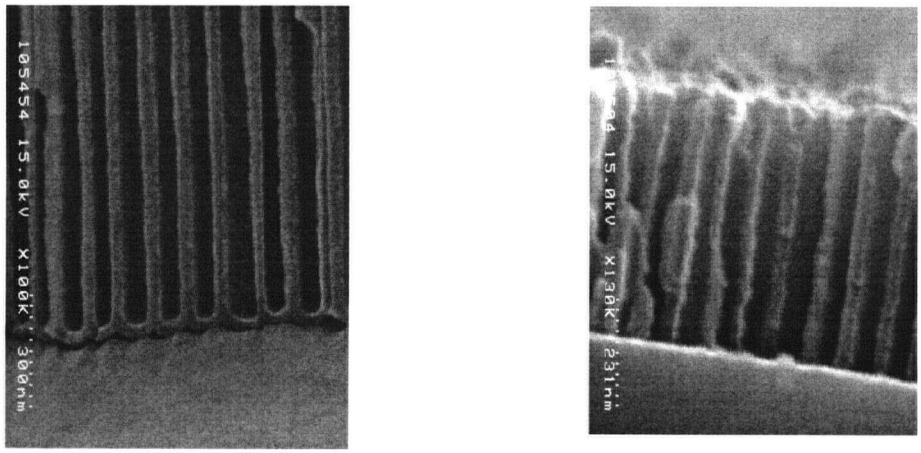

Figure 2.3 SEM images of cross-section (a) a porous alumina film on Al substrate with an alumina barrier layer of ~30 nm (image obtained by Dr. Katja Rademacher) and (b) on porous alumina film on Si, showing pores etched down to the Si substrate.

2.3.3 Polymer Incorporation into Porous Alumina Films

In this work, the luminescent polymers MEH-PPV, DP-PPV, DP_{10}-PPV are incorporated into porous alumina films via an adsorption method similar to that used by Tolbert *et al.*[37] to incorporate polymers into nanoporous silica. With porous alumina films on Al, the incorporation of the orange-red MEH-PPV was visible by eye due to the relative thickness of the alumina film. After immersing the treated alumina film in the polymer solution for two days, it was washed thoroughly by immersing the sample in fresh THF four times for one minute each. After this process the anodized area appears orange whereas the surrounding non-anodized Al was shiny and not coloured. The THF rinses are important to remove any loosely adsorbed polymer from the alumina layer. The same method was employed to incorporate polymer into the alumina on Si films, however, the MEH-PPV was not visible by eye in the thinner samples. Under irradiation with UV-light (λ= 366 nm), a faint orange emission was observed in the anodized area on these samples.

Similar observations were obtained from incorporation of DP-PPV into porous alumina on both Si and Al substrates. When the alumina sample was immersed in the polymer precursor solution in THF, the anodized area did not change in appearance by eye. However, upon conversion to the conjugated polymer by heating to approximately 280 °C, the anodized area turned a deep yellow colour. For incorporation of DP_{10}-PPV, the anodized area did not change in appearance by eye after immersion in the polymer solution. However, under irradiation with UV light, the anodized area appeared green. This was the case for the alumina films on both Si and Al substrates. These results

clearly demonstrate that these polymers all adsorb strongly to the alumina. The interaction between the relatively non-polar polymers and the polar porous alumina wall is important since it may affect the electronic and optical behaviour, as well as the conformation of the polymer within the host. SEM images were taken before and after polymer incorporation, however, the pore diameters do not change significantly in these images, nor are the pores visibly "plugged" (Figure 2.4).

(a) (b)

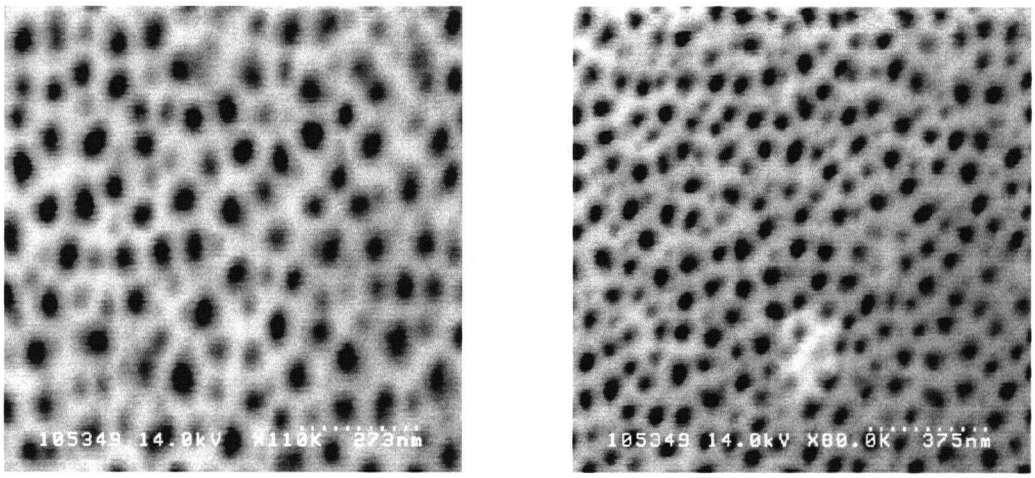

Figure 2.4 SEM images of a porous alumina film on Si (a) before polymer incorporation and (b) after polymer incorporation.

These images, however, must be interpreted carefully since the pores are not uniform; so it is difficult to accurately determine if there are significant changes in pore diameter. Since the images obtained before and after polymer incorporation were taken at different spots on the surface, direct comparison of pore diameters is not possible. Fluorescence micrographs were also obtained to determine the distribution of the polymer in the pores. A cross-sectional view (Figure 2.5), shows that the entire porous alumina layer is emissive under irradiation from 455 nm to 480 nm. Fluorescence microscopy of a porous

alumina film on Si showed fluorescence from a 1 μm layer, which corresponds to the thickness of the Al layer deposited initially (Figure 2.6).

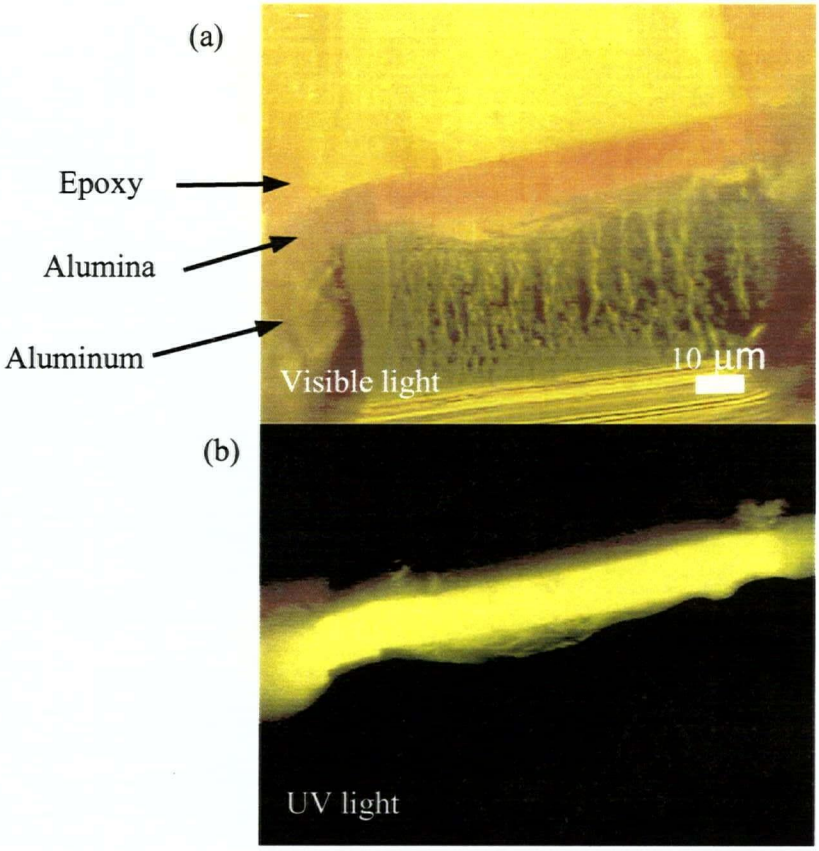

Figure 2.5 Cross-sectional view of porous alumina containing MEH-PPV under (a) visible and (b) UV light (images obtained by Dr. Katja Rademacher).

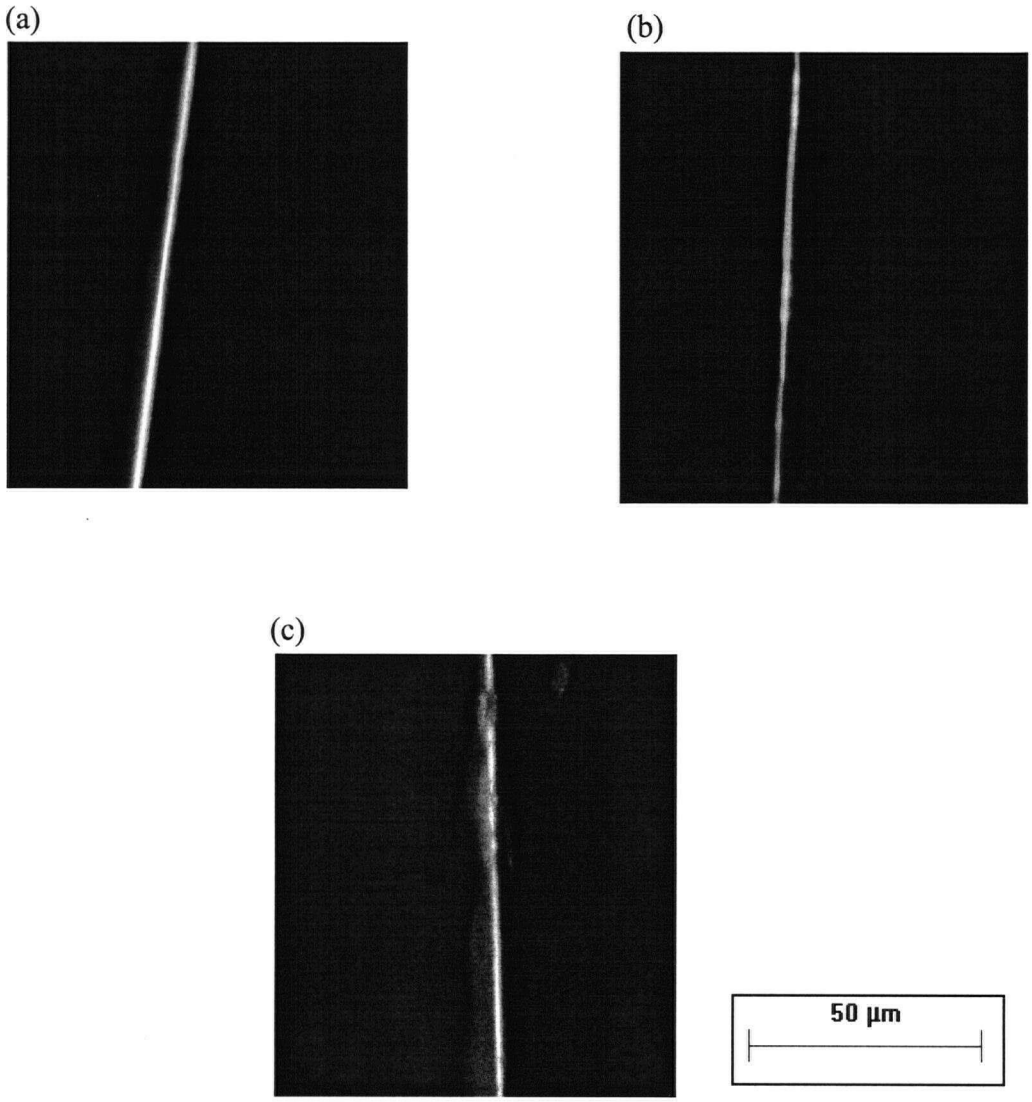

Figure 2.6 Fluorescence micrographs at 50x magnification of cross sections of (a) MEH-PPV, (b) DP-PPV and (c) DP_{10}-PPV in porous alumina on Si. The white areas indicate fluorescent regions.

Care must be taken when assessing the significance of these images since photobleaching as well as the difficulty in obtaining good resolution for such a small sample size will affect the intensity of fluorescence observed.

As mentioned previously, SEM images of the pores before and after polymer incorporation do not show significant changes. This supports the conclusion that a thin layer of polymer adsorbs to the pore walls. Indeed, this has been previously observed for other polymers on alumina particles. SEM images of *in situ* polymerized poly(maleic acid-1-octadecene) on alumina particles also do not indicate a significant change in particle diameter, suggesting a monolayer coating.[38]

2.3.4 Proposed Mechanism of Polymer Incorporation to Porous Alumina Films

As mentioned previously, the fact that the polymer cannot be removed from the alumina host by repeated rinsing with THF indicates that strong, irreversible adsorption of the polymers to the porous alumina occurs. It is reasonable that the interaction of the Lewis acidic Al centers of the porous alumina and the Lewis basic phenyl groups of the polymer result in this strong adsorption (Figure 2.7). This type of interaction with aromatic groups has also been observed for other low valent metals such as Ti.[9] The interaction involves the empty π-orbitals on the Lewis acidic Ti and the filled π-orbitals on the Lewis basic phenyl rings. In addition, surface hydroxyl groups on the pore walls can act as Bronsted acids which can also interact with the phenyl groups of the aromatic backbone.[39,40,41] The Lewis acidic centers are more rigid and demand a certain bonding geometry in order for favourable interactions to occur.[39] The Bronsted acid sites are more flexible, allowing for the polymer to adsorb onto the pore walls with different

geometries. Finally, in the case of MEH-PPV, the polymer may adsorb via the alkoxy groups in a fashion analogous to the adsorption of polyethylene oxide, (PEO) on alumina particles (Figure 2.8).[41]

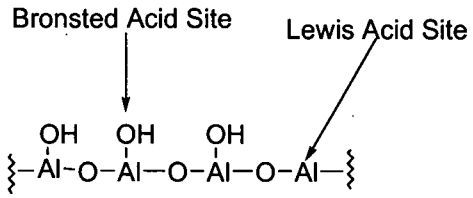

Figure 2.7 Bronsted and Lewis acid sites on the pore walls of alumina.

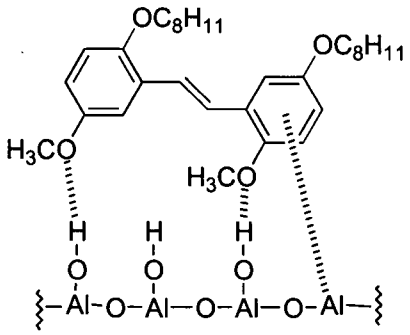

Figure 2.8 Bonding between Lewis acid sites on porous alumina and Lewis basic sites on MEH-PPV.

The solvent from which the polymer is adsorbed is very important and is expected to affect the orientation of the adsorbed polymer. In THF, MEH-PPV is known to be coiled with the alkoxy groups pointing out towards the solvent while the polymer backbone is pointed inward to minimize unfavourable non polar/ polar interactions.[42,43] It is possible that the polymer is first anchored to the pore walls via the alkoxy groups, and these interactions are then strengthened as the polymer backbone comes into contact with the pore walls.

With DP-PPV, the polymer precursor containing a chlorine group adsorbs initially and the polymer is then thermally converted to the conjugated form. This precursor polymer may coil or aggregate in such a way that the chlorine groups point outward toward the solvent during the adsorption process. DP-PPV was adsorbed to the porous alumina from THF and toluene solutions. By eye, it appears that more DP-PPV adsorbs from toluene than THF. This may be due to differences in polymer morphology in the two solvents. In THF, the chlorine groups are expected to face outward, reducing the amount of Lewis acid/Lewis base interactions with the alumina surface. In toluene, the chlorine groups most likely face inward, with the aromatic groups on the backbone interacting with the alumina surface, thus facilitating the interactions between the Lewis basic phenyl rings and the Lewis acid Al centers, resulting in stronger adsorption.

2.3.5 Attempts to Increase Polymer Loading

In an attempt to increase the polymer loading in the alumina films, the polymer solution was heated to 60 °C during the adsorption process for one day. To the eye, samples prepared in this way were equally intense in colour as when the sample was prepared at room temperature. With heating, the rate of polymer adsorption is faster than at room temperature, possibly because the polymer uncoils and enters the pores more easily. It was also attempted to increase polymer loading by slowly evaporating the solvent during adsorption, thus gradually increasing the concentration in solution with the goal of depositing more polymer into the pores. However, these samples appear to be identical to samples that were not treated in this manner.

2.4 Summary and Possible Future Work

Porous alumina films were grown on Al, Si, and ITO substrates. Three luminescent polymers were incorporated into the alumina films via an adsorption process from THF solution. The proposed adsorption process involves Lewis acidic sites on the pore walls of the alumina and the Lewis basic sites on the polymer backbone. The solvent used may play an important role in the adsorption process, since the morphology of the polymer will differ in different solvents. In chlorobenzene, MEH-PPV is known to be in a more extended, uncoiled form whereas in THF, MEH-PPV is more coiled up to reduce the polar-non-polar interactions between the polymer backbone and the ether group of THF.[43] Further investigation into the effects of the solvent on the adsorption process would be useful. As well, studies into the effects of pore diameter are needed. As the pore size decreases, the polymer loading is expected to increase due to the larger available surface area per unit volume. However, using smaller pores may also result in difficulties in coaxing the polymer into the pores particularly if it is coiled. Members of the PPV family are not the only polymers that are highly luminescent and studies into encapsulation of other classes of luminescent polymers such as polythiophenes or poly (9-vinyl carbazole)s (PVK) could be investigated. Polymers with different structures may result in different adsorption processes and loading as the Lewis acid/ base interactions will differ.

Chapter 3

Investigations into the Nature of the Interaction between Polymer and the Pore Walls

3.1 Introduction

In Chapter 2, the incorporation of the luminescent polymers: MEH-PPV, DP-PPV and DP_{10}-PPV into porous alumina via adsorption from solution was described. Several factors are expected to impact on the intensity of the observed luminescence from the resulting hybrid materials, including the amount of polymer incorporated, the effectiveness of the pores to offer protection to the polymer from atmospheric oxygen and the nature of the polymer/pore wall interaction. As discussed in Chapter 2, the interactions between the conjugated polymers and the alumina walls are believed to involve bonding between Lewis acidic and Lewis basic sites. The nature of the polymer-pore wall interaction may be expected to affect the amount of polymer incorporated. In untreated alumina, the pore walls are polar due to the surface hydroxyl groups. It is possible to reduce the polarity of the walls by functionalization with compounds such as alkyldimethylchlorosilanes or aryldimethylchlorosilanes (Figure 3.0). It is possible that modifying the pore walls in this way would alter the amount of polymer which adsorbs, since this would result in an increase in non-polar/non-polar interactions, and a decrease in Lewis acid/Lewis base interactions.

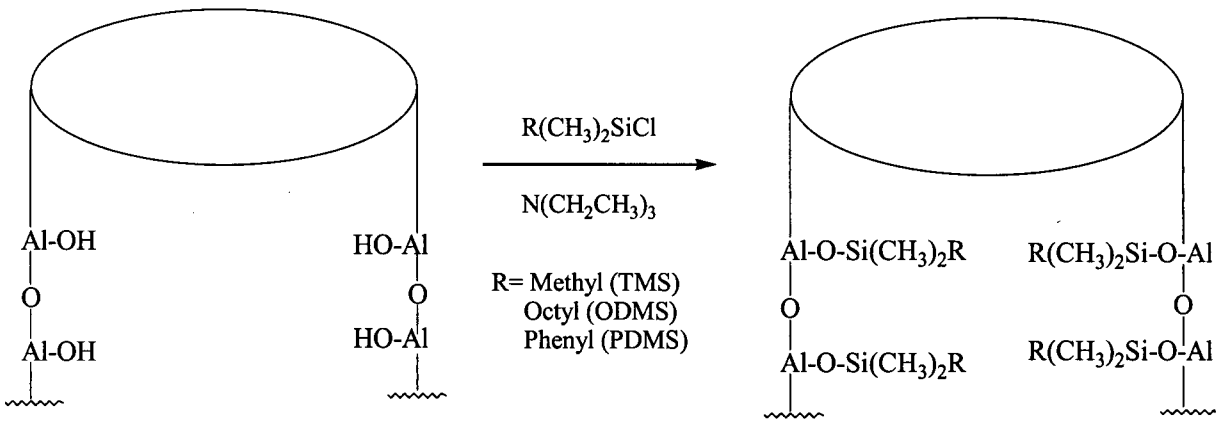

Figure 3.0 Silanization of porous alumina.

In this Chapter the extent of polymer incorporation in the hybrid materials, the degradation of MEH-PPV adsorbed to porous alumina and the interactions of the polymer with the pore walls will be explored. Silanization of the alumina with trimethylchlorosilane (TMS), octyldimethylchlorosilane (ODMS) and phenyldimethylchlorosilane (PDMS), allow the effect of changes in the polarity of the pore walls on polymer adsorption to be probed.

3.2 Experimental Details

3.2.1 General Details

All equipment and chemicals used are the same as those described in Section 2.2, with the following additions: TMS, ODMS and PDMS were purchased from Aldrich and used without further purification. Hexanes were distilled from benzophenone ketyl/sodium/tetraglyme and triethylamine was distilled from calcium hydride. Porous alumina membranes (Anodisc 13) were purchased from VWR Whatman. UV-vis measurements were obtained on an ATI Unicam UV2 Spectrophotometer. Fluorescence spectra were obtained on a Fluorolog Fl3-222 spectrometer, using a sample holder built for the author by the mechanical shop in the Department of Chemistry at UBC. The sample holder consisted of a plastic block with a backing plate held at 45° to the incident light and detector, which holds a quartz plate. The samples was sandwiched between two quartz plates and held in place by taping the quartz plates together. The excitation wavelength (λ_{ext}) used for MEH-PPV was 480 nm and for DP_{10}-PPV, was 400 nm. X-ray photoelectron spectroscopy was done by Dr. Ken Wong at the Interfacial Analysis and Reactivity Laboratory at UBC.

3.2.2 Attempted Extraction of MEH-PPV Adsorbed to Anodisc Membrane

Three methods were attempted to extract MEH-PPV from the Anodisc membrane:

Method A. An MEH-PPV treated Anodisc membrane was immersed in a vial containing concentrated H_3PO_4 for 3 hours in order to dissolve the porous alumina. The remaining insoluble material was diluted with water and extracted first with diethyl ether, then with THF. The vial and the separatory funnel were washed thoroughly first with ether and then THF. The resulting organic solution was concentrated by rotary evaporation and the residue was dried under vacuum. A THF solution (10 mL) of this material was prepared and an UV-vis spectrum was taken. A similar procedure was used for the dissolution of porous alumina using 1 M NaOH and 5% w/w H_3PO_4.

Method B: Under nitrogen, a MEH-PPV treated Anodisc membrane was placed in the thimble holder of a Soxhlet extractor. THF was used to extract soluble material from the Anodisc membrane for three days.

Method C: An MEH-PPV treated Anodisc membrane was immersed in a vial containing chloroform. The sample was sonicated for one hour with frequent changes of the solvent This procedure was repeated using methylene chloride, ethyl acetate and silicon-based oil.

3.2.3 UV-vis Spectroscopy of MEH-PPV Adsorbed to Anodisc Membranes

MEH-PPV was adsorbed to Anodisc membranes following the procedure outlined in Section 2.2. The samples were then dried under nitrogen in the dark. To examine the effects of air and light, the samples were placed on a quartz plate and held in place with Scotch tape. Some of the samples were then irradiated with UV-light (λ_{ext} = 366 nm) in air and the absorbance spectrum of the samples monitored over the course of five hours

irradiation time. Other samples were irradiated under an inert atmosphere by placing them in a nitrogen filled glass box. Other samples were treated similarly but kept in the dark.

3.2.4 Silanization of Anodisc Membranes

Anodisc samples were first placed under vacuum in a test tube with a sidearm, and heated to 100 °C for two days. The samples was then placed under a nitrogen atmosphere, and triethylamine (0.1 mL) and TMS (1 mL) were added to the tube. The solution was mixed and allowed to stand at room temperature for 2 hrs, after which time the excess TMS was removed under reduced pressure. The sample was then washed with hexanes (3 x 2 mL), dried under nitrogen and then heated to 100 °C for one hour. The sample was then washed with distilled water and ethanol and dried under vacuum. The same procedure was followed for treatment with phenyldimethylchlorosilane (PDMS) and octyldimethylchlorosilane (ODMS). The adsorption of the polymers to the silanized Anodisc membranes follows the procedure described in Section 2.2.

3.3 Results and Discussion

3.3.1 Porous Alumina Membranes

A convenient way to probe the interaction between the adsorbed polymer and the pore walls is to study thin films of the composite material without an underlying substrate. Using such substrates, methods such as transmission UV-vis spectroscopy can be used since the porous alumina does not absorb in the visible light and thus should not interfere with such measurements. For this reason, we have chosen a commercially available filter membrane, Anodisc 13 (Figure 3.1) for the work described in this

Chapter. These membranes are 60 μm thick; most of the membrane (58 μm) has a pore diameter of 200 nm and the remaining 2 μm has a pore diameter of 20 nm.[44] These membranes are prepared electrochemically from Al substrates where the anodization voltage is reduced gradually when the desired thickness is reached.[45] This allows for separation of the alumina films from the underlying substrate. These membranes have been used previously in various other studies including as a template to grow nanowires,[46] and studies involving protein adsorption to membranes.[47]

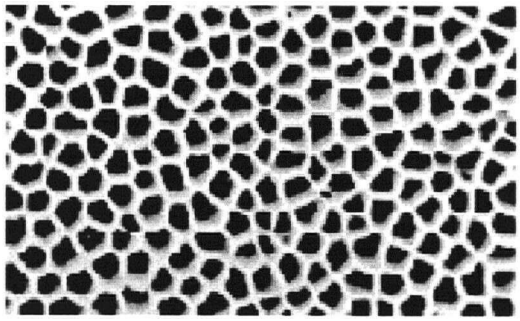

Figure 3.1 SEM image of pores on Anodisc membrane.[48]

3.3.2 Degree of Polymer Adsorption

In order to determine the amount of polymer adsorbed from solution, several attempts were made to separate the polymer from the host alumina with the goal of quantifying the amount of polymer via UV-vis spectroscopy. The first approach involved dissolving the porous alumina host using either acid or base, which should leave the polymer behind. Concentrated H_3PO_4 was found to dissolve the Anodisc membrane in three hours. Since the use of concentrated acid is rather harsh and may react with the polymer, milder conditions, 5% w/w H_3PO_4 and 1 M NaOH were also tried. The dissolution time is longer (three days) when 5% w/w H_3PO_4 was used and shorter (one

hour) when 1 M NaOH was used. Under these conditions, some coloured polymer was left behind in addition to some white particles. In a control experiment, a MEH-PPV film was cast on a glass slide and was immersed in the acid or base solutions. After a few hours small white needles were also found in the solutions. The white material was insoluble in water but soluble in organic solvents such as THF. The UV-vis (absorbance) spectrum of the extracted polymer was blue shifted relative to that of a freshly prepared MEH-PPV solution in THF (Figure 3.2). This is an indication that some degradation of the polymer occurs, resulting in a reduction in conjugation length. Blue shifts have been previously observed in other studies for example upon photo-oxidation and cleavage of conjugated polymers, leaving shorter, less-conjugated fragments.[49] Since any degradation would result in errors in the quantification, this method of determining polymer loading was not pursued further.

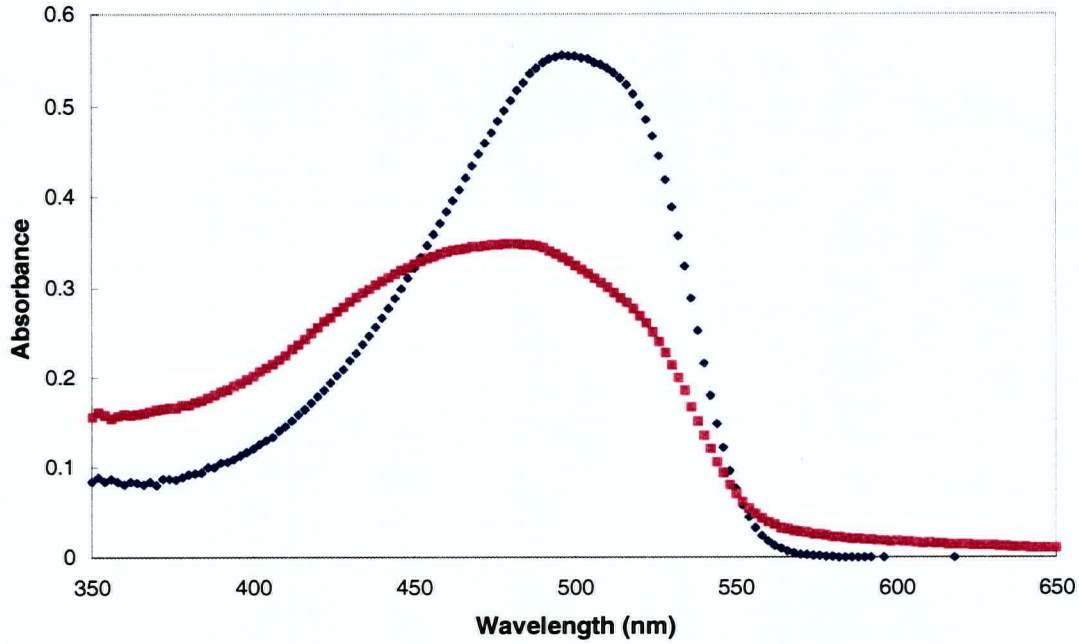

Figure 3.2 UV-vis absorption spectra of freshly prepared MEH-PPV (◆) and MEH-PPV recovered from Anodisc in THF (■).

A second approach to quantifying the amount of adsorbed polymer involved extraction of the polymer from the membrane with a solvent. A Soxhlet extraction was used with THF as the solvent and the MEH-PPV treated Anodisc membrane was placed in the thimble holder of the extractor. This extraction was carried out under nitrogen for three days, after this time, the membrane was still orange, indicating that the extraction was not complete. This attempt was therefore also abandoned.

A third attempt was made in which the polymer-treated Anodisc membrane was sonicated with frequent solvent changes. Several solvents were tried including chloroform, methylene chloride, ethyl acetate and a silicon-based oil. After one hour of sonication, the membrane was still coloured, again indicating incomplete removal of the polymer.

3.3.3 Effect of Light and Air on Polymer Adsorbed to the Anodisc Membrane

To assess the effect of UV-light and air on the polymer-alumina hybrid materials, MEH-PPV treated Anodisc membranes were irradiated with UV-light in air and under nitrogen. Another set of samples was kept in the dark both in air and under nitrogen. The membranes were held in place with tape on quartz slides and measurements were taken over the course of 5 hours. The sample irradiated in air showed a blue shift of 5 nm in λ_{max} over the course of the experiment. For all the other samples, a smaller blue shift of 2 nm was observed over the experiment. A blue shift in λ_{max} is an indication of the degradation of the polymer due to a reduction in the conjugation length.[49] Figure 3.3 shows a normalized plot of the absorbance at λ_{max}. The data indicates that there is a substantial decrease in the absorption at λ_{max} for the sample which is irradiated in air. In comparison, membranes kept under nitrogen and in the dark show much lower decreases. Thus, in order for the type of degradation of the polymer to occur which results in a decrease in the absorbance intensity, both light and air must be present.

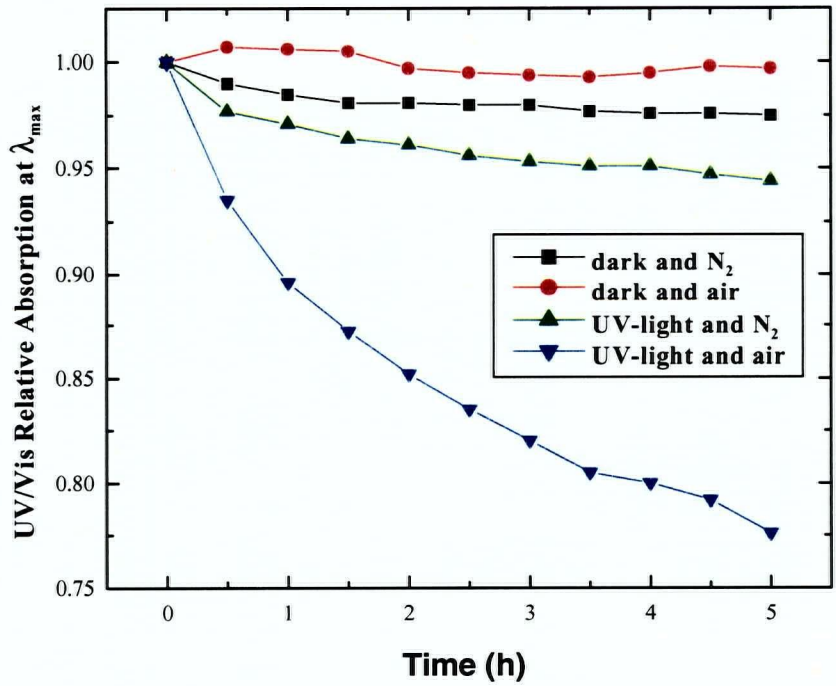

Figure 3.3 Normalized plot of UV-vis absorbance at λ_{max} as a function of time for MEH-PPV/Anodisc membrane hybrids.

Degradation studies on thin films of MEH-PPV were done by Atreya and coworkers.[49] Their study involved 50-70 nm thick MEH-PPV films, spin-cast from xylene on a glass substrate. In this study, a large blue shift (95 nm) and broadening of the peak was observed after continuous irradiation through Pyrex at λ_{ext} = 260-400 nm for 5 hours. A considerable decrease in absorption intensity at λ_{max} was also observed, however quantification of this decrease over the course of the experiment was not reported. They found that when the irradiation is carried out under an argon atmosphere, the large decrease in absorption intensity and blue shift was not observed. Their result suggests that air is needed for the polymer to degrade rapidly. These results are consistent with our degradation studies on the polymer-treated Anodisc membranes. There are, however, some differences between the Atreya study and the hybrid materials

studied here which are important to note. A greater blue shift in λ_{max} was observed for the Atreya study possibly due to the higher lamp power (150 W) used in comparison to our studies (6 W), leading to a faster rate of photo-oxidation. Most significantly, in the hybrid materials all the polymer is on the surface and exposed directly to air. In contrast, the bulk thin-films consist of a small amount of "surface" material. A complete comparison of the effect of light/air is therefore difficult unless it is carried out under carefully controlled conditions.

3.3.4 Polymer-Pore Wall Interactions

Silanization of the polar pore walls was used to modify the nature of the interior of the pores, in order to examine the effect of polymer adsorption. Several considerations must be taken into account with this process. The number of surface hydroxyl groups will influence the silanization process. In silica,[50] the surface hydroxyl groups are not uniformly distributed and this can also be expected for porous alumina. A survey of the literature revealed many studies of the effects of silanization on silica surfaces,[47,50-55] however little is reported about the modification of alumina, we thus extrapolate the reactivity of hydroxyl groups on alumina from the known behaviour of silica. For the silanization of silica surfaces, a catalyst such as an amine, is often used. The role of the catalyst is to decrease reaction times as well as being directly involved in the chemistry of the silanization process. When the catalyst is used, an island-type growth of the silanized area on the surface results, where silanization occurs in a localized area of the surface and then spreads, eventually giving the maximum bonding density of the silane.[51,52] Without the catalyst, a random distribution of the silane on the surface is

attained, which ultimately does not result in the maximum bonding density. The catalyst forms hydrogen bonds with the surface hydroxyl groups. The reaction between the silane and the surface hydroxyl groups results in the release of the amine which then hydrogen bonds to the closest available hydroxyl group. This allows the adjacent silane to then react with the hydroxyl group at the hydrogen-bonded amine (Scheme 3.0).

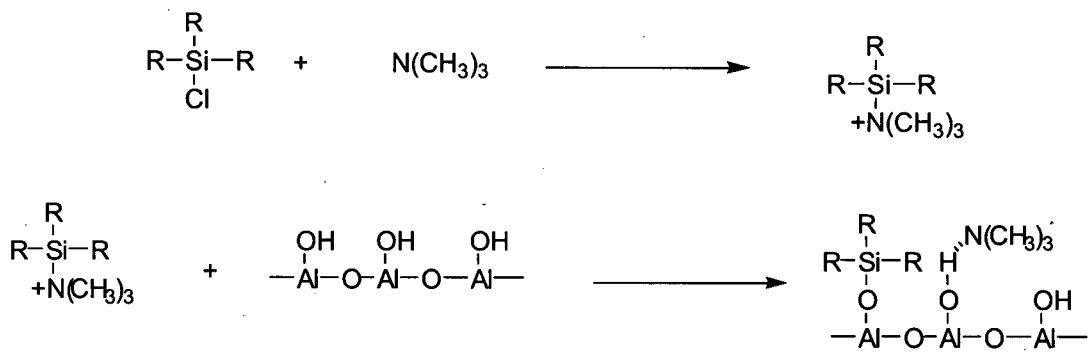

Scheme 3.0

The choice of silane is also an important factor; monochlorosilanes were chosen over di- or trichlorosilanes due to their reactivity. Monochlorosilanes have only one mode of surface bonding (since only one Si-Cl bond is present), whereas di- or trichlorosilanes can bond via 1-3 bonds to the surface or even polymerize by reacting with other silane molecules (Scheme 3.4).[53] The silanes that were selected for this study to probe the interactions of the polymer and the pore walls were trimethylchlorosilane (TMS), octyldimethylchlorosilane (ODMS) and phenyldimethylchlorosilane (PDMS). With these different silanes, the bonding density is expected to differ due to steric considerations.[46,47,54] A silane with very short alkyl chains such as TMS is expected to

have a high bonding density on the surface. However, with ODMS and PDMS, the bonding density is not expected to be as high due to the greater steric demands of the long alkyl chains and the phenyl group. Because of the lower likelihood that every surface hydroxyl group is silanized with ODMS and PDMS, a random silanization process is most likely for these silanes. This should lead to a lower bonding density and less uniformity of surface functionalization.

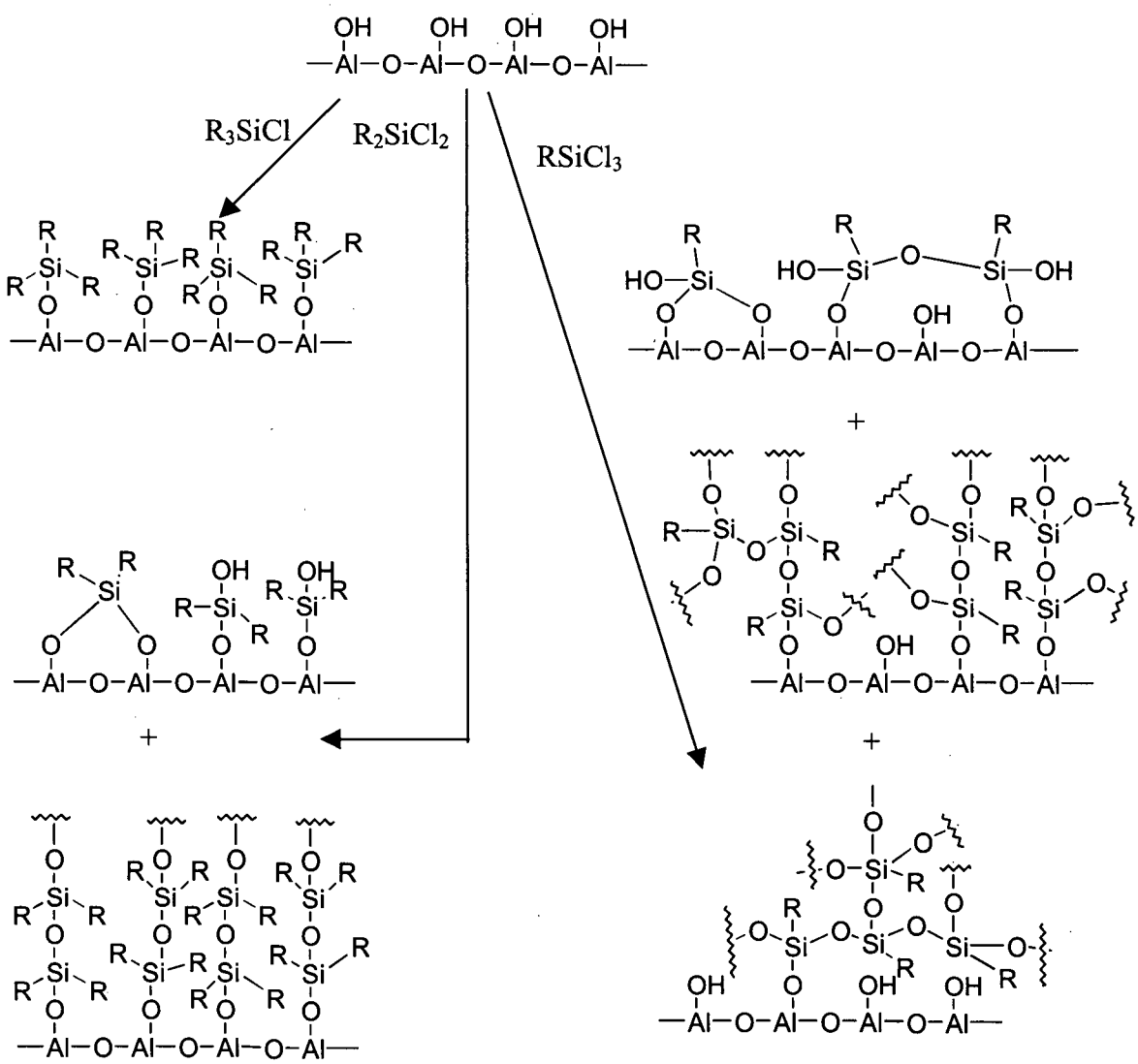

Figure 3.4 Possible bonding modes with mono, di and trichlorosilanes with alumina surfaces.

Another factor that must be considered, especially for ODMS and PDMS, is the surface morphology. On a flat surface, an equilibrium exists between the extended, brush-like form and the flopped over, coiled form, (Figure 3.5).[51]

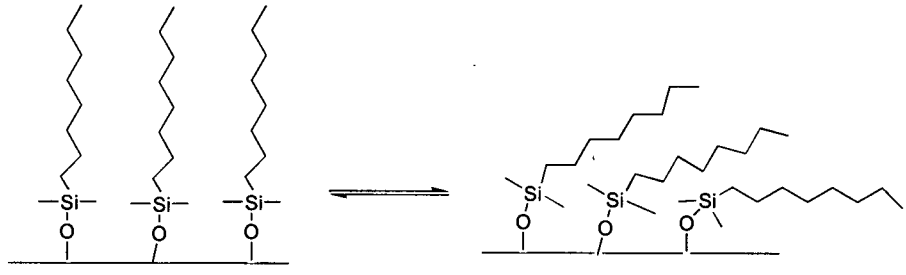

Figure 3.5 Surface morphology of a silane monolayer.

However, on a curved surface, such as within the pores of porous alumina, the area available for the silane is reduced and the possibility of the layer being in the fully extended conformation may be limited.[51,52] For pore diameters of approximately 5 nm, and with alkyl chains longer than eight carbons, the equilibrium will be shifted towards the coiled conformation so that the alkyl chains can fit into the pores, resulting in a corresponding decrease in bonding density.[51,52] With the relatively larger pore sizes that are used in the work described in this thesis, this is not a significant factor and the silanes are thus expected to be in equilibrium between the two conformations shown in Figure 3.3.

Surface reflection IR spectroscopy at a grazing angle of 30° on the porous alumina on silicon substrates was attempted to characterize the silanized samples. The

only peak that was evident in the IR spectra that was different from the spectrum of non-silanized porous alumina on silicon was at 1260 cm^{-1} (Figure 3.6). This is attributed as a Si-C stretch. The Si-O stretch was not observed, however would fall in the same range as the broad Al-O stretch (1040 cm^{-1}). Other stretches (C-H, C-C) were also obscured by the strong Al-O absorptions. These reflectance IR spectra are similar to the reflectance IR of porous alumina reported by Wackelgard.[56] Transmission IR was also attempted on porous alumina on Si, however, a regularly sinusoidal wave was observed in these spectra. This was also present in the transmission IR experiments carried out by Klaus *et al.*[44] on Anodisc membranes. The origin of this sinusoidal wave is not known, but it may be related to the periodicity of the pores.

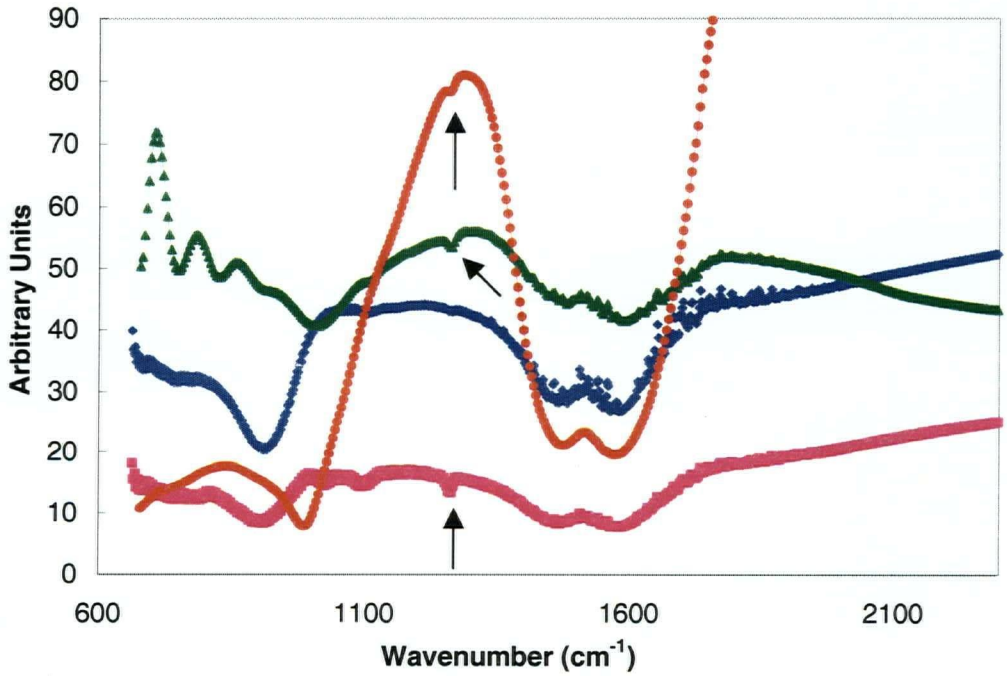

Figure 3.6 Surface reflectance IR spectra of (a) non-silanized (◆), (b) TMS(■), (c) PDMS (●)and (d) ODMS (▲) silanized porous alumina on Si at a grazing angle of 30 °. Arrows indicates the new band at 1260 cm^{-1}.

X-ray photoelectron spectroscopy (XPS) was also used to characterize the silanized materials. For all silanes used, the XPS spectrum of the silanized alumina did not contain a peak due to chlorine suggesting that no residual trialkylchlorosilane remained. Both Al and O were present and the binding energies for these elements matches those reported for alumina (75 eV for Al 2p and 532 eV for 1s O).[57] The Al and O signals dominate the spectrum and no substantial shifts in the binding energy for Al and O peaks are expected. Significantly a Si 2p peak was present in the spectrum of all the samples indicating that silanization was successful (Figure 3.7). The binding energy of this peak is ~ 99.7 eV, close to the Si 2p peak reported for organosilanes (~100 eV).[57]

(a)

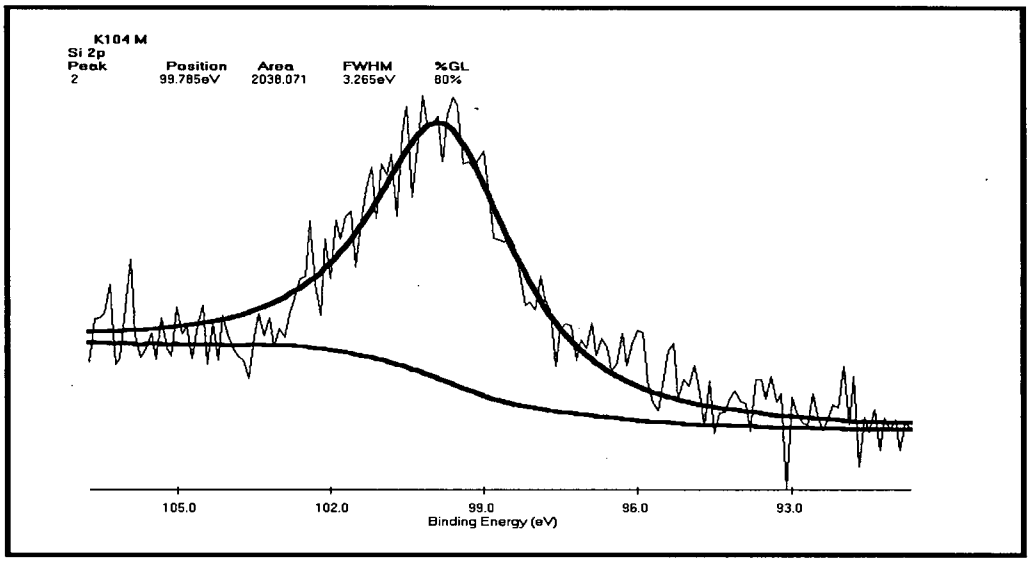

(b)

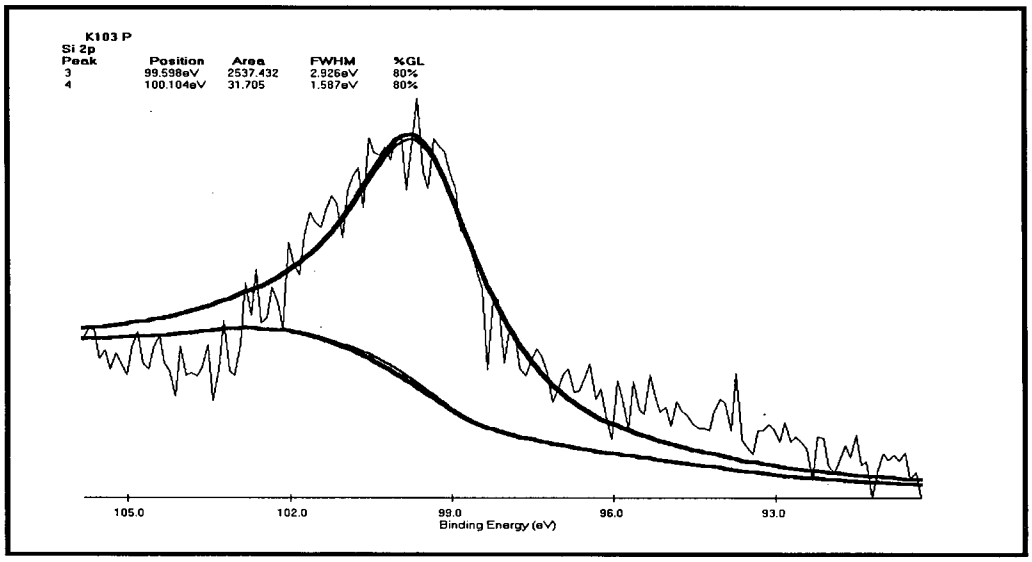

(c)

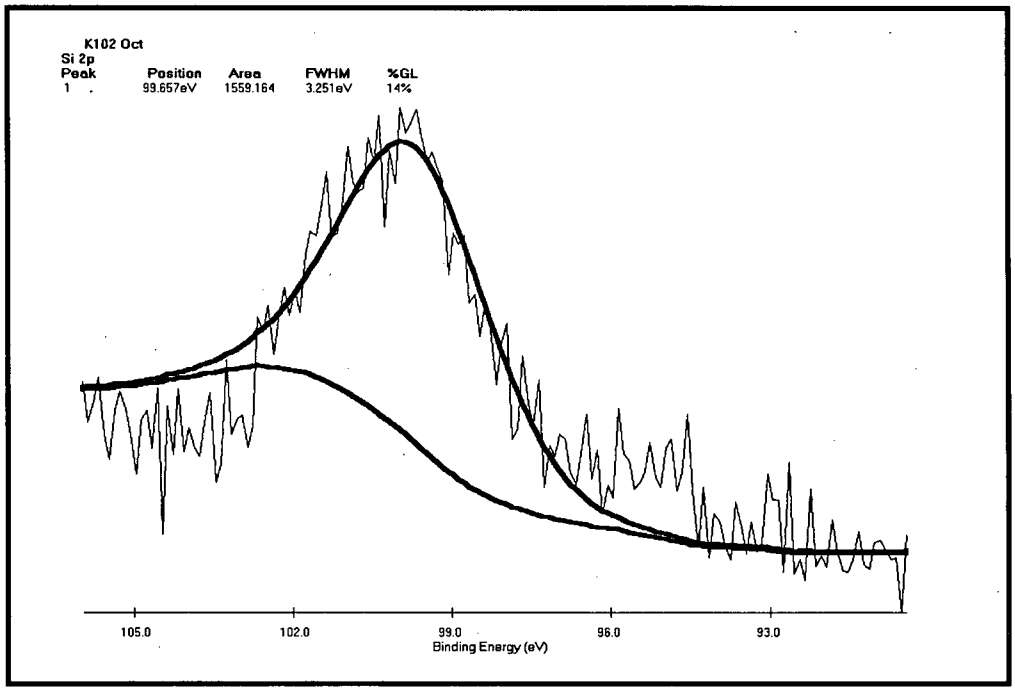

Figure 3.7 Si (2p) region of XPS spectra for (a) TMS, (b) PDMS and (c) ODMS silanized Anodisc membranes.

SEM images of the pores before and after silanization did not reveal any substantial change in pore diameter, nor was any "plugging" of the pores on the surface observed (Figure 3.8).

(a) (b)

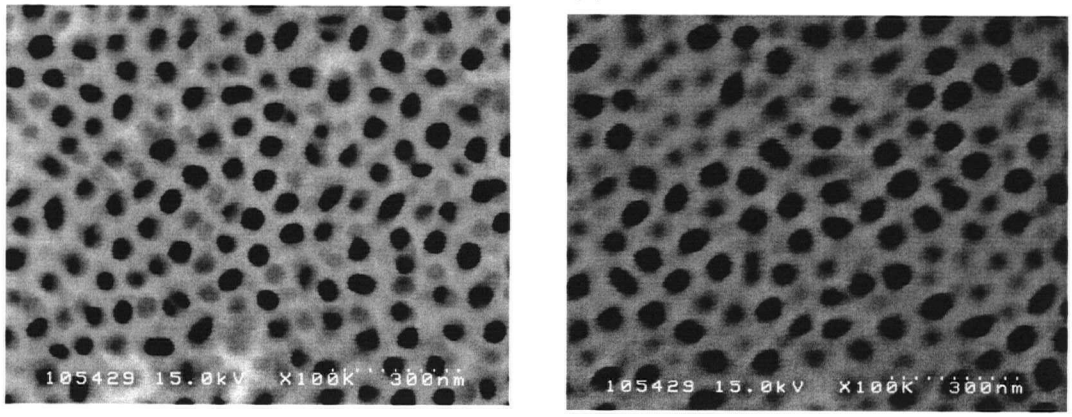

Figure 3.8 SEM images of (a) non-silanized and (b) TMS silanized porous alumina on Si.

When polymer is adsorbed into silanized membranes, there also does not appear to be a significant difference in SEM images between silanized pores without polymer and with polymer (Figure 3.9)

(a) (b)

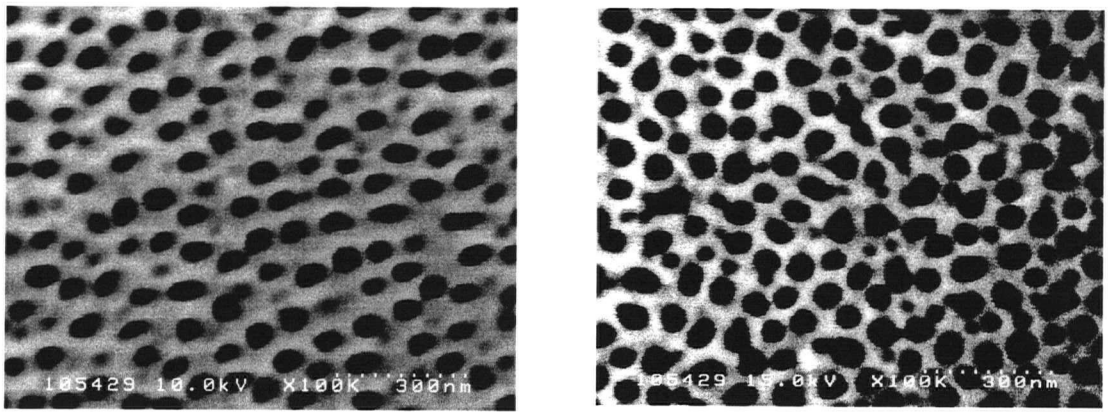

Figure 3.9 SEM images of TMS silanized porous alumina (a) without polymer and (b) with MEH-PPV adsorbed.

Those observations are consistent with a thin, absorbed coating of the polymer on the walls of the pores rather than fully or partially filled pores. In these experiments, the samples were vigorously rinsed to remove any polymer which may be loosely trapped within the pores. UV-vis measurements were then taken to determine the relative amount of polymer adsorbed to silanized and non-silanized Anodisc membranes (Figure 3.10).

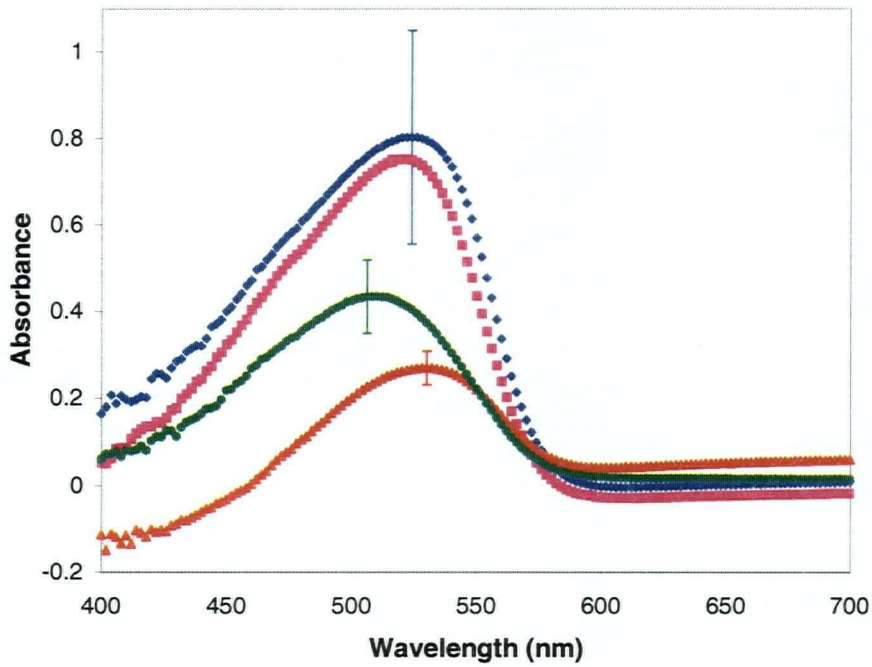

Figure 3.10 UV-vis spectra of non-silanized (◆) and TMS (■), ODMS (▲) and PDMS (●) silanized Anodisc membranes with MEH-PPV adsorbed.

These measurements show that the amount of adsorbed polymer in the ODMS and PDMS silanized alumina was less than in the non-silanized and TMS silanized samples. These differences may be related to the interactions of the polymer with the alumina walls. In the non-silanized pores, the Lewis basic polymer and the Lewis acidic Al centres interact (*vide supra*). However, this interaction is lessened due to screening by

the alkyl and aryl groups when the pores are silanized. Silanization blocks the Al centers and surface hydroxyl groups with hydrocarbon and aromatic groups. When the polymer does not adsorb strongly, it is easier to remove during the rinsing process, lowering the amount of polymer remaining in the pores. There are also differences in loading between alumina samples silanized with different silanes. The TMS derivatized membrane shows a similar loading to the non-silanized Anodisc whereas the ODMS and PDMS deriviatized samples contain less polymer than the TMS silanized Anodisc membranes. Many factors may influence the amount of polymer adsorbed. The surface bonding densities differ between silanes affecting the interactions between the polymer and pore walls. TMS has the highest bonding density due to its small size as discussed previously. Thus, the amount of adsorbed polymer may be expected to be lower than for ODMS and PDMS silanized Anodisc membranes due to less available Lewis acid sites in these samples. However, the opposite effect is observed, possibly due to the large substituent groups in ODMS and PDMS, which better prevent interactions with the pore wall. The methyl groups are smaller and any defects or non-uniformity in the silanized surface will allow for easier access to the Lewis acid centers. As well, the different conformations of ODMS (extended and flopped-over forms) could cover up any surface defects, preventing polymer access to the Lewis acid sites.

To determine if the modification of the interior of the pores has any effect on the photoluminescence of the polymer, fluorescence spectroscopy was used. Polymer treated Anodisc membranes were placed in a holder with a 45° quartz backplate and sandwiched between two quartz slides and the holder was held in place with tape. In measuring the fluorescence spectra of the samples, errors can arise due to several effects. The location

of the irradiated area on the sample and any movement of the sample holder can affect the measured fluorescence intensity. Thus, every effort must be taken to keep these factors constant between measurements. As well, degradation of the polymer with repeated scans was found to affect the fluorescence intensity. Finally, authentic sample-to-sample variation can affect the experiment.

The fluorescence spectra indicate that for MEH-PPV treated samples, the highest fluorescence intensity is observed for non-silanized Anodisc membranes (Figure 3.9). This is likely due to a higher loading of polymer in the non-silanized case over the others as observed by absorbance measurements (*vide supra*). Within the series of silanized samples, the ODMS and PDMS silanized Anodisc membranes have similar fluorescence intensities, but are both higher than in the TMS silanized material. These differences may be due to differences in the morphology of the polymer within the pores. For example, it is possible that adsorbed polymer incorporated in the ODMS and PDMS silanized samples may have reduced interchain interactions, leading to higher fluorescence intensities than in the TMS case. When comparing the fluorescence intensities with the UV-vis absorbance for the same samples, it appears that overall the fluorescence intensity is enhanced for the PDMS and ODMS treated material over the TMS treated material. This may be due to better polymer alignment and packing in these samples.

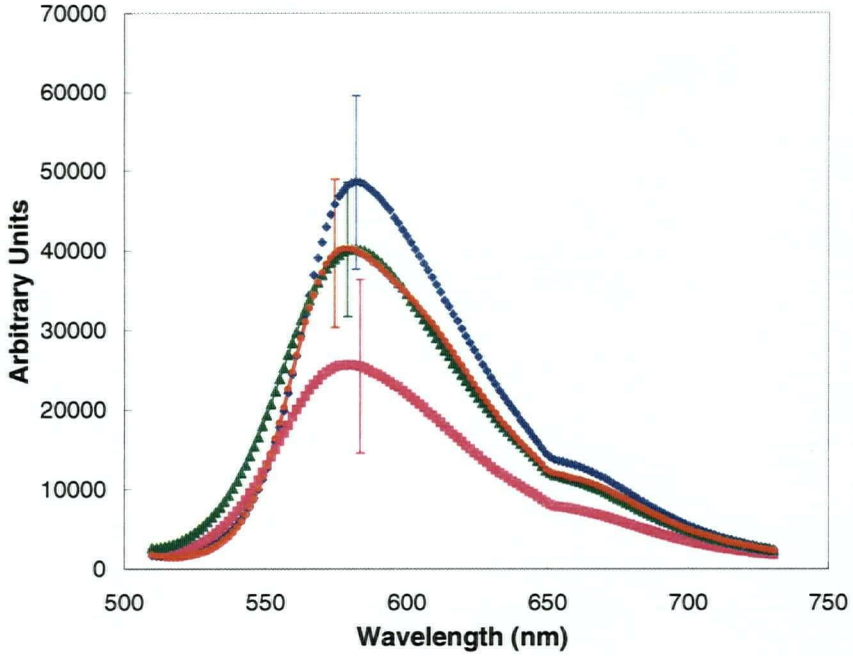

Figure 3.11 Fluorescence spectra of non-silanized (◆) and TMS (■), PDMS (●) and ODMS (▲) silanized Anodisc membranes with MEH-PPV adsorbed.

In these spectra, the errors were calculated from the standard deviation of two separate samples over 10 scans. In Figure 3.11, only the error at λ_{max} is shown. Clearly the large errors in these measurements make it difficult to make unambigous conclustions from this data.

With DP_{10}-PPV, the fluorescence spectra indicate that the non-silanized Anodisc has the highest fluorescence intensity, followed by the PDMS, ODMS and the TMS silanized samples (Figure 3.12). This provides further information regarding how the polymer may be interacting with the pore walls. The phenyl groups of the PDMS may be involved in favourable π-interactions with the phenyl groups in the polymer. In the ODMS and TMS silanized samples, the alkyl chains may act to separate the polymer

chains, leading to unfavourable aggregation or stacking. This would then be expected to lead to lower fluorescence intensity.

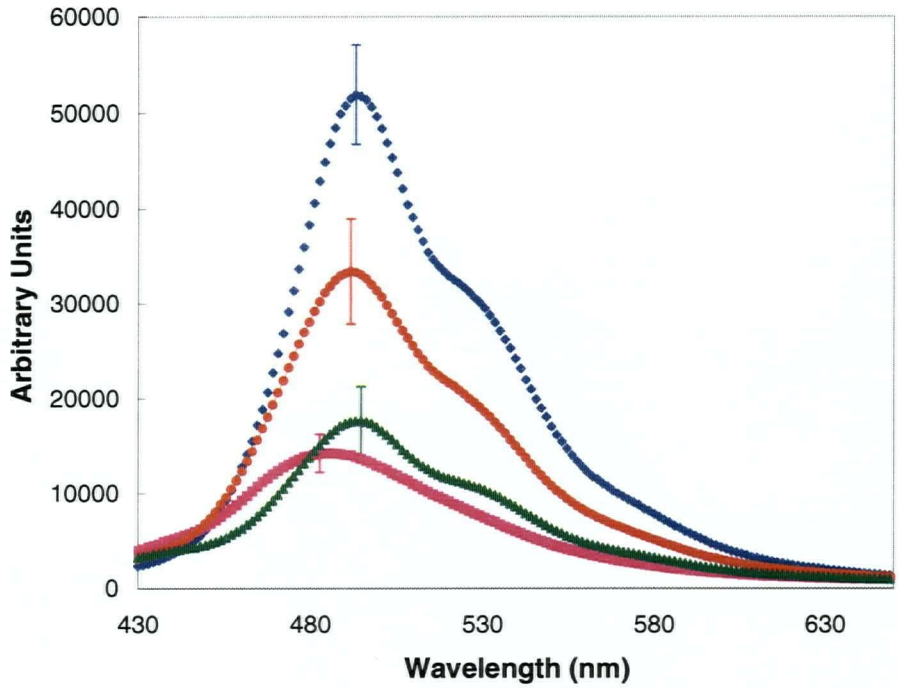

Figure 3.12 Fluorescence spectra of non-silanized (◆) and TMS (■), ODMS (▲) and PDMS (●) silanized Anodisc membranes with DP_{10}-PPV adsorbed.

The errors were calculated for the DP_{10}-PPV treated Anodisc membranes using the same method as for the MEH-PPV treated membranes. In Figure 3.11, the error at λ_{max} is also shown. The errors in this data are smaller than those found for the MEH-PPV experiments. This may be an indication that MEH-PPV is less stable than DP_{10}-PPV.

3.4 Conclusions and Future Work

The extent of polymer incorporation could not be determined directly due to difficulties in extracting the polymer from the Anodisc membranes. The use of Anodisc membranes allowed for degradation studies with UV-vis spectroscopy. Irradiation with

UV light under air causes a rapid decrease in absorption intensity in comparison to samples irradiated under nitrogen. Degradation studies should be done in the future on silanized porous alumina to which polymers have been adsorbed to determine if the oxygen in the porous alumina is involved. Silanization of the pore walls was shown to alter the interactions between the polymer and pore walls, by changing the degree of screening of the Lewis acidic Al centres from the polymer. Hydrophobic interactions did not result in an increase polymer incorporation. Within the different silanes used, differences in absorbance and fluorescence intensity for silanized samples treated with polymer were observed. These differences are attributed to differences in bonding density, steric effects of the silane within the pores, and possible aggregation of the polymer. The silanization studies were done on Anodisc membranes, in the future; these studies could be repeated on porous alumina films on other substrates.

Chapter 4

Summary and Suggestions for Future Work

The encapsulation of luminescent polymers from the PPV family into a nanoporous host material has been successfully demonstrated. Polymer adsorption is believed to be occur due to interactions between Lewis acidic sites on the pore walls and Lewis basic sites on the polymers. By modifying the pore walls with trialkylchlorosilane groups, the polarity of the pore interiors may be modified. This affects the polymer loading due to screening of the Lewis acidic sites. For MEH-PPV the degree of loading from absorption spectroscopy was found to be in the order: non-silanized > TMS > ODMS, PDMS silanized Anodisc membrane. From fluorescence intensities, the order was found to be non-silanized > ODMS, PDMS > TMS. For adsorbed DP_{10}-PPV, the fluorescence intensities are in the order: non-silanized > PDMS > ODMS, TMS. Direct quantification of polymer loading is difficult and attempts made to quantify the amount of MEH-PPV in the pores were unsuccessful.

This host-guest approach towards materials for organic LEDs is promising, however, much work remains to be done on this system. The use of other hosts, the effects of solvent, the extent of polymer protection in a silanized host, the morphology of the polymer in the host as well as the quantification of the amount of polymer in the host are very important issues that still need to be probed. Finally, device fabrication using these encapsulated materials will ultimately determine if these devices are better than the currently available ones.

With improvements to LEDs, the incandescent light bulb invented over a century ago is slowly becoming obsolete. LEDs have found applications in flat panel displays, automobile lights, and outdoor lighting.[1] Organic and polymeric materials have emerged as promising candidates for LEDs and will play a major role in the development of

second generation LEDs. Although there are still problems with these materials that impact on commercial viability, whoever manages to overcome them stands to capture a multi-billion dollar industry.

References

1. M. George Craford, Visible Light-Emitting Diodes: Past, Present, and Very Bright Future, *MRS Bulletin* **2000**, *25* (10), 27-32.

2. Segura, J. L., *Acta Polym.* **1998**, *49*, 319-344.

3. Sheats, J.R; Chang, Y.L; Rotiman, D.B.; Stocking, A.; *Acc. Chem. Res.* **1999**, *32*, 193-200.

4. Sheats, J.R.; Antoniadis, H.; Hueschen, M.; Leonard, W.; Miller, J.; Moon, R.; Roitman, D.; Stocking, A.; *Science* **1996**, *273*, 884-888.

5. West, A.R; *Solid State Chemistry and it's Applications;* John Wiley and Sons Oxford, England 1984; Chapter 14.

6. Fletcher, R.; *Optics and Photonics News* **April 1999**,19-23.

7. Friend, R. H.; Gymer, R.W.; Burroughes, J. H.; Marks, R. N.; Taliani, C.; Bradley, D.D.C.; Dos Santos, D. A.; Bredas, J. L.; Lögdiund, M.; Salaneck, W. R.; *Nature* **1999** , *397*, 121-128.

8. Heeger, A.J.; *Solid State Communications* **1998**, *107* (11), 673-679.

9. Rothberg, L. J.; Yan, M.; Kwock, E. W.; Miller, T.M.; Galvin, M. E.; Son, S.; Papadimitrakopoulos, F.; *IEEE Transactions on Electron Devices* **1997**, *44* (3), 1258-1261.

10. Cao, Y.; Parker, I.D.; Yu, G.; Zhang, C.; Heeger, A.J.; *Nature* **1999**, *397* (4), 414-417.

11. Rothberg, L. J.; Yan, M.; Son, S.;Galvin, M.E.; Kwock, E. W.; Miller, T. M.; Katz, H. E.; Haddon, R.C.; Papadimitrakopoulos, F.; *Synth. Met.* **1996**, *78*, 231-236.

12. Brown, A.R.; Bradley, D.D.C.; Burroughes, J. H.; Friend, R. H.; Greenham, N. C.; Burn, P. L.; Holmes, A. B.; Kraft, A.; *Appl. Phys. Lett.* **1992**, *61* (23), 2793-2795.

13. Kraft, A.; Grimsdale, A.C.; Holmes, A. B.; *Angew Chem. Int. Ed* **1998**, *37*, 403-428.

14. Chang, W.P.; Whang, W. T.; Lin, P.W.; *Polymer* **1996**, *37* (9), 1513-1518.

15. Neef, C. J.; Ferraris, J. P.; *Macromolecules* **2000**, *33*, 2311-2314.

16. Kim, S.H.; Chu, H. Y.; Zyung, T.; Do, L. M.; Hwang, D. H.; *Synth. Met.* **2000**, *111-112*, 253-356.

17. Papadimitrakopoulos, F.; Zhang, X.M.; Thomsen, D.L.; Higginson, K. A.; *Chem. Mater* **1996**, *8*, 1363-1365.

18. Jakubiak, R.; Rothberg, L. J.; Wan, W.; Hsieh, B.R.; *Synth. Met.* **1999**, *101*, 230-233.

19. Jakubiak, R.; Collison, C.J.; Wan, W. C.; Rothber, L.J.; Hsieh, B.R.; *J. Phys. Chem A.* **1999**, *103*, 2394-2398.

20. Scott, J.C.; Kaufman, J.H.; Brock, P. J.; DiPietro, R.; Salem, J.; Goitia, J. A.; *J. Appl. Phys.* **1996**, *79* (5), 2745-2751.

21. Yan, M.; Rothberg, L. J.; Kwock, E. W.; Miller, T.M.; *Phys. Rev. Lett.* **1995**, *75* (10) 1992-1995.

22. Carter, S.A.; Angelopoulos, M.; Karg, S.; Brock, P. J.; Scott, J. C.; *Appl. Phys. Lett.* **1997,** *70* (16), 2067-2069.

23. Chiavarone, L.; Di Terlizzi, M.; Scamarcio, G.; Babudri, F.; Farinola, G.M.; Naso, F.; *Appl. Phys. Lett.* **1999**, *75* (14), 2053-2055.

24. Burrows, P. E.; Bulovic, V.; Forrest, S. R.; Sapochak, L. S.; McCarty, D. M.; Thompson, M. E; *Appl. Phys. Lett*, **1994**, *65*, 2922-2924.

25. Yamashita, K.; Mori, T.; Mizutani, T.; *J. of Phys D. Appl. Phys*, **2001**, *34*,740-743.

26. Diggle, J. W.; Downie, T. C.; Goulding, C. W.; *Chem. Rev.* **1969**, *69*, 395-403.

27. Keller, F.; Hunter, M. S.; Robinson, D. L.; *J. of Electrochem. Soc.* **1955**,*100* (9), 411-419.

28. Li, A.P.; Muller, F.; Birner, A.; Nielsch, K.; Gosele, U.; *Adv. Mat.* **1999**, *11* (6), 483-487.

29. Masuda, H.; Hasegwa, F.; *J. of Electrochem. Soc.* **1997**, *144* (5), L127-L130.

30. Li, F.; Zhang, L.; Metzger, R.; *Chem. Mater.* **1998**, *10*, 2470-2480.

31. Thompson, G. E.; *Thin Solid Films* **1997**, *297*, 192-201.

32. Crouse, D.; Lo, Y.H.; Crouse, M.; Miller, A.E.; *Appl. Phys. Lett.* **2000**, *76* (1), 49-51.

33. Gruzinskii, V.V.; Kukhto, A. V.; Mozalev, A. M.; Surganov, V. F.; *J. Appl. Spec.* **1997**, *64* (4), 497-502.

34. Wan, W.C.; Antoniadis, H.; Choong, V.E.; Razafitrimo, H.; Gao, Y.; Feld, W.A.; Hseih, B.R.; *Macromolecules* **1997**, *30*, 6567-6574.

35. Masuda, H.; Yada, K.; Osaka, A.; *Jap. J. Appl. Phys.* **1998**, *37* (pt 2. 11A), L1340-L1342.

36. Wolf, M.O; Abraham-Pattanyus, A.G.; unpublished results, 2001

37. Wu, J.; Gross, A.F.; Tolbert, S.H.; *J. Phys. Chem. B* **1999**, *103*,2374-2384.

38. Mao, Y.; Fung, B.M.; *Chem. Mater.* **1998**, *10*, 508-517.

39. Van der Beek, G. P.; Stuart, M.A.C.; Fleer, G.J.; Hofman, J.E.; *Macromolecules* **1991**, *24* (25), 6600-6611.

40. Chen, M.H.; Furusawa, K.; *Langmuir* **1996**, *12*,2015-2018.

41. Mathur, S.; Moudgil, B.M.; *Minerals and Metalluragical Processing* **1998**, *15* (2), 24-28.

42. Yang, Y.; Liu, J.; Shi, Y.; *J. Appl. Phys.* **2000**, *87* (9), 4254-4262.

43. Nguyen T. Q.; Doan, V.; Schwartz, B.J.; *J. Chem. Phys.* **1999**, *110* (8), 4068-4078.

44. Ott, A.W.; Klaus, J.W.; Johnson, J.M.; George, S.M.; McCarley, K.C.; Way, J. D.; *Chem. Mater.* **1997**, *9*, 707-714.

45. Schwanbeck, H.; Schmidt, U.; *Electrochimica Acta* **2000**, *45*, 4389-4398.

46. Garcia, J.M.; Asenjo, A.; Velázquez, J.; Garcia, D.; Vázquez, Aranda, P.; Ruiz-Hitzky, E.; *J. Appl. Phys.* **1999**, *85* (8), 5480-5482.

47. Matinez, F.; Martin, A.; Prádanos, P.; Calvo, J.I.; Palacio, L.; Hernández, A.; *J. Coll. and Interface Sci.* **2000**, *221*,254-261.

48. http://www.2spi.com/catalog/spec_prep/filter2.html

49. Atreya, M.; Li, S.; Kang, E.T.; Neoh, K.G.; Ma, Z.H.; Tan, K.L.; Huang, W.; *Polymer Degradation and Stability* **1999**, *65*, 287-296.

50. Boksányi, L.; Liardon, O.; Kováts, E.; *Adv. Coll. and Interface Sci.* **1976**, *6*, 95-137.

51. Staroverov, S.M.; Fadeev, A.Y.; *J .Chrom.* **1991**, *544*, 77-98.

52. Kinkel, J.N.; Unger, K.K.; *J. Chrom.* **1984**, *316*, 193-200.

53. Fadeev, A.Y.; McCarthy, T. J.; *Langmuir* **2000**, *16*, 7268-7274.

54. Berendsen, G.E.; Pikaart, K.A.; de Galan, L.; *J. Liq. Chrom.* **1980**, *3* (10), 1437-1464.

55. Claudy, P.; Letoffé, J.M.; Gaget, C.; Morel, D.; Serpinet, J.; *J. Chrom.* **1985**, *329*, 331-339.

56. Wackelgard, E.; *J. Phys: Condens. Mat.* **1996**, *8*, 4289-4299.

57. Muilenberg, G. E. (editor); Moulder, I. F.;, Davis, L.E.; Riggs, W.H.; Wagner, C.D.; *Handbook of X-ray Photoelectron Spectroscopy*; Perkin-Elmer Corporation, 1979.